Synthesis of Satellite and Surface Measurements, Model Results, and FRAPPÉ Study Findings to Assess the Impacts of Oil and Gas Emissions Reductions on Maximum Ozone in the Denver Metro and Northern Front Range Region in Colorado

Patrick Reddy[1]

[1]Affiliation not available

March 9, 2023

Synthesis of Satellite and Surface Measurements, Model Results, and FRAPPÉ Study Findings to Assess the Impacts of Oil and Gas Emissions Reductions on Maximum Ozone in the Denver Metro and Northern Front Range Region in Colorado

Patrick J. Reddy[1]

[1]Independent Research Scientist.

Corresponding author: Patrick J. Reddy (preddyresearch@gmail.com)

Key Points:

- Correlations between ozone and methane, ethane, and oil and gas emissions are high in the north and lower in the south of the study region.
- Spatial gradients in correlations and trends in maximum O_3 match gradients in modeled oil and gas contributions.
- Regression and Bayesian correlation suggest that 67% of O_3 from O&G VOCs has been eliminated at northern sites between 2012 and 2019.

Abstract

The Denver Metro/Northern Front Range area has been designated a Severe nonattainment area for O_3. Previous research associated with the 2014 FRAPPÉ field campaign and a 2017 O_3 source apportionment modeling analysis point to north-south gradients in oil and gas (O&G) impacts on O_3, with greater contributions to the north and a dominance of mobile sources to the south. Recent analysis of AIRS satellite methane enhancement and ethane trends in the area show ~50% and ~70% reductions in methane and ethane, respectively, from 2013-2020. These are consistent with reductions in O&G VOC emissions estimated in the most recent O_3 State Implementation Plan but inconsistent with a timeline of top-down methane flux estimates for limited periods from 2012-2021. Reductions in annual fourth maximum eight-hour O_3 concentrations from 2012 to 2019 are 5 ppb greater at Fort Collins West (FTCW) to the north than at Chatfield Reservoir to the south. Bayesian correlation analyses and partial correlations between FTCW O_3 and ethane conditioned for OMI tropospheric NO_2 suggest that most of the 9-ppb reduction here is due to declines in O&G emissions, and 9 ppb is comparable to estimated O&G VOC contributions on high-concentration days in the northern portion of the study area. The gradient in trends suggests that significant O&G emissions reductions have benefited locations in the central and northern portions of the nonattainment area. Monitor footprint modeling helps to explain the relative influence of the O&G emissions at key sites.

1 Introduction

Using surface and satellite measurements, results from air quality field campaigns and studies, emissions inventories, and monitor footprint modeling, this study considers evidence for declines in O_3 associated with reductions in O&G emissions. It represents a simple synthesis of empirical data and existing information to track progress in reducing O_3 associated with emissions from O&G sources. Given the abundance of complex research on O_3 for this region, this synthesis may serve as a more accessible indicator for policy makers assessing recent progress and possibly as a starting point for future research as well. Two major 2014 summer field campaigns, the National Center for Atmospheric Research (NCAR) and State of Colorado Front Range Air Pollution and Photochemistry Éxperiment (FRAPPÉ) and the National Aeronautics and Space Administration (NASA) Deriving Information on Surface conditions from Column and Vertically Resolved Observations Relevant to Air Quality study (DISCOVER-AQ) were conducted simultaneously in northern Colorado and are key to our understanding of patterns in summer O_3 photochemistry and transport (Flocke et al., 2020; Crawford and Pickering, 2014).

The Denver Metro/North Front Range (DM/NFR) region of northern Colorado is classified as a Severe and Moderate nonattainment area (NAA) for the 2008 and 2015 O_3 National Ambient Air Quality Standards (NAAQS) of 75 ppb and 70 ppb, respectively (links to Federal Register announcements for 2022 reclassifications are provided in the Open Research section). Compliance with these standards is measured by the three-year average of the annual fourth maximum daily eight-hour average (DMAX8). The three-year average is referred to as the design value. Attainment of these standards is challenging because the DM/NFR contains a large metropolitan area with diverse urban sources of O_3 precursors as well as the Wattenberg Field O&G resource area. The Wattenberg Field, which has the densest concentration of O&G extraction facilities within the wider Denver Julesburg Basin (DJ Basin), is the top O&G production area in Colorado and one of the most productive in the US. In addition, estimated

2017 background O_3 transported into Colorado on high-concentration days accounted for 73%-77% (52 ppb to 55 ppb) of DMAX8 at FTCW, RFLAT, NREL, and CHAT (Ramboll Environ and Alpine Geophysics, LLC., 2017). This high background contribution creates a significant challenge for local and state air quality regulators since the fraction of total O_3 contributed by sources within the DM/NFR is small. Reddy and Taylor (2022) briefly summarize the history of VOC emissions reduction measures implemented for O&G sources in the area.

As of 2020, nine monitors in the DM/NFR were out of compliance with the 2015 NAAQS for O_3 (Regional Air Quality Council, 2022). The focus of this paper is on O_3 at five high-concentration sites, Fort Collins West (FTCW), Rocky Flats North (RFLAT), the National Renewable Energy Laboratory (NREL), Chatfield Reservoir (CHAT), and the Weld County Tower (WCT) located in the Wattenberg Field O&G resource area north of Denver. Site locations and the boundaries of the NAA are plotted in Figure 2. The 2020 design values at FTCW, WCT, RFLAT, NREL, and CHAT were 75 ppb, 70 ppb, 79, ppb, 80 ppb, and 81 ppb, respectively (Regional Air Quality Council, 2022).

All of the sites except WCT are high-concentration sites classified as urban scale or representative of an area of 4 to 50 km in size (Colorado Department of Public Health and Environment Air Pollution Control Division, 2022a). WCT is a high-concentration neighborhood scale monitor, which means it is representative of an area 0.5 to 4 km in scale. The other four high-concentration sites are downwind of precursor source areas, and O_3 production has had time to increase concentrations on route to the monitors under thermally-driven upslope flow (Pfister et al., 2019). This flow regime is the typical transport condition on high-concentration days (Flocke et al., 2020; Pfister and Flocke, et al., 2017; Reddy and Pfister, 2016).

Pfister and Flocke et al. (2017) indicate that mobile and O&G sources are the largest contributors to local summer O_3 in 2014, each contributing 30-40% to the fraction associated with DM/NFR emissions on high-O_3 days. Both O&G and mobile sources appear to contribute 6-10 ppb to average DMAX8. They indicate that O&G sources have a greater influence in the northern portions of the DM/NFR while mobile sources have a greater influence in the southern section which includes Denver. Based on a 2011 modeling and meteorology framework and 2017 emissions, Ramboll Environ and Alpine Geophysics, LLC. (2017) show a pronounced north-south gradient in O&G contributions to DMAX8. O&G contributions peak at 7.0 ppb at WCT and are only 1.7 ppb at CHAT in the southern section of the NAA. These are the average contributions for the 10 highest modeled days at each site. McDuffie et al. (2017) conclude that O&G volatile organic compounds (VOC) could account for 6 ppb of O_3 on photochemically active days, based on modeling and trace gas measurements collected at the Boulder Atmospheric Observatory tower (BAO) in July and August of 2012. The BAO is within the Wattenberg Field and in what I will refer to as the northern portion of the NAA (see Figure 2). Based on these studies, reductions in O&G emissions would be expected to result in greater reductions in O_3 to the north. On high concentration days in the northern portion of the NAA, we could expect ~6-10 ppb of O_3 production from O&G sources in the 2012-2017 timeframe.

Using surface measurements and data from the NASA Atmospheric Infrared Sounder (AIRS) instrument, Reddy and Taylor (2022) found 55% and 73% reductions in local methane enhancement (over background) and ethane, respectively, from 2013-2020. They concluded that ethane measurements at the Platteville site in the Wattenberg Field are representative for this

O&G field and that ~70% of area methane was from O&G sources in 2012. Lyu et al. (2021) show that ethane and non-methane hydrocarbons at Platteville are largely from O&G sources from 2013-2016. The study area defined by Reddy and Taylor (2022) is a grid cell that includes most of the emissions sources in the NAA, Denver, Boulder, Greeley and much of the Wattenberg Field; and they refer to it as the Denver-Denver Julesburg Basin (DDJB). They attributed these reductions to state emissions control regulations for O&G VOC sources as well as voluntary changes made by the O&G industry. These reductions occurred even though oil production increased by 343% and gas production by 297% from 2012-2020. In contrast, when the results from several short-term, top-down methane flux studies for the DJ Basin are considered on a timeline, they show a slight declining trend from 2012-2021 (Petron et al., 2014; Peischl et al., 2018; Cusworth et al., 2022; Fried et al., 2022; Riddick et al., 2022). Possible reasons for discrepancies in methane trends will be discussed.

If there has been a ~70% reduction in O&G VOC emissions between 2013 and 2019, then we would expect to see reductions in peak O_3, especially in those areas in the NAA where O_3 contributions from O&G emissions are high. The analysis presented here explores patterns and trends in annual fourth maximum 8-hour O_3 to see if there have been decreases consistent with changes in O&G emissions and to differentiate the influences of VOCs and NO_x using partial correlations and Bayesian correlation metrics. Platteville morning ethane is used as a surrogate or tracer for O&G VOCs.

2 Data Sources and Methods

2.1 Data Sources

NASA AIRS satellite-derived annual DDJB methane enhancement data for June-August 2011-2020 and median annual Platteville ethane for 2012-2020 were acquired from a data repository (Reddy and Taylor, 2022b) created in support of the paper by Reddy and Taylor (2022). In the current study these are compared with annual fourth maximum O_3 and O&G VOC emissions estimates to determine if decreases in O&G VOC emissions are reflected in O_3 trends. They used June through August AIRS Version 7 retrievals for the 700 hPa level for 2003-2020 (Goddard Earth Sciences Data and Information Services, 2019) for a grid cell that includes much of the O_3 precursor source area within the DM/NFR. The grid cell is 1° by 1° and centered on 40°N and 105°W. AIRS methane data are available on the NASA Giovanni site. Enhancements above background were calculated by subtracting June-August mean methane from the NOAA Global Monitoring Laboratory (GML) Niwot Ridge (NWR) high-altitude background site (Dlugokencky, 2021). NWR is at 40.05°N, 105.59°W, and 3,523 m above sea level (MSL). The derivation of the AIRS DDJB methane enhancement which is based on the 700 hPa level product is described fully by Reddy and Taylor (2022), and they conclude that it is proportional to and representative of methane within the summer boundary layer.

The Platteville monitor is at 40.21°N, 104.82°W, and 1,469 m MSL (see Figure 2), and the rationale for using annual median Platteville ethane is described in detail by Reddy and Taylor (2022). Three-hour samples of VOCs and ethane were collected at Platteville from 6 to 9 a.m. every six days with full years of data collection beginning in 2012. Annual estimated emissions data for O&G VOCs in the NAA for years beginning in 2011 were obtained from a 2022 O_3 State Implementation Plan (SIP) technical support document (Colorado Department of Public

Health and Environment Air Pollution Control Division, 2022b). Estimates of O&G, on-road mobile (OR), non-road mobile (NR), and electric generating unit (EGU) contributions to O_3 in the NAA were taken from Ramboll Environ and Alpine Geophysics, LLC. (2017) and the online local source apportionment tool based on their work (see Open Research and Acknowledgements sections). They used 2017 emissions to model source contributions to DMAX8 on the top 10 modeled days in 2011 at FTCW, WCT, RFLAT, NREL, and CHAT.

Annual fourth maximum and DMAX8 O_3 concentrations were obtained from the Environmental Protection Agency (EPA) and the Colorado Department of Public Health and Environment (CDPHE). These were used to track trends and relationships with other variables from 2010-2019. Data for the year 2020 was not used because of frequent wildfire smoke (Albores et al., 2023; Flynn et al., 2021). Data were acquired for the FTCW, WCT, RFLAT, NREL, and CHAT sites. FTCW is 1,571 m above sea level (MSL) at 40.59°N, 105.14°W; WCT is 1,484 m MSL at 40.39°N, 104.74°W; RFLAT is 1,802 m MSL at 39.91°N, 105.19°W; NREL is 1,832 m MSL at 39.74°N, 105.18°W; and CHAT is 1,676 m MSL at 39.53°N 105.07°W. The annual fourth maximum DMAX8 used here are based on rankings after removal of events flagged for wildfire smoke or stratospheric intrusions of O_3. The recalculated values are more likely to track with changes in local emissions.

To test for the effects of meteorology on trends in O_3, June-August mean 500 hPa heights were acquired from the National Center for Environmental Prediction (NCEP) Reanalysis for a 2.5° by 2.5° grid cell centered on 40°N 105°W which contains the DM/NFR. The NCEP Reanalysis meteorological data product is described by Kalnay et al. (1996). Reddy and Pfister (2016) found that July monthly mean surface O_3 concentrations in the DM/NFR are strongly correlated with July 500 hPa heights. Reddy et al. (2020) subsequently used annual fourth maximum concentrations that are strongly correlated with mean June-August 500 hPa to correct trends in fourth maximum concentrations.

Both NO_x and VOCs are key O_3 precursors. Each needs to be considered to assess the possible effects of decreases in O&G VOC emissions. Pfister et al. (2019) determined that carbon monoxide and methane contribute ~2 ppb and ~1 ppb of O_3 in the area, respectively, with the highest contributions in the mountains to the west. Tracking trends in the complex of factors governing carbon monoxide and methane contributions as well as other primary and secondary precursors is beyond the scope of this study. Previous studies show that OMI NO_2 can be used in assessments of surface O_3 and that OMI tropospheric NO_2 correlates well with surface NO_2 (Vazquez Santiago et al., 2021; Paraschiv et al., 2017). Tropospheric NO_2 has a lifetime of 2-5 hours in the summer and 12-24 hours in the winter, and as a result it is well-correlated with local emissions (Goldberg et al., 2021).

Annual average satellite-derived tropospheric NO_2 data from the Ozone Monitoring Instrument (OMI) were obtained for the DM/NFR region from the NASA Giovanni website for 2012 and 2019. These were used for the maps in Figure 3 and 4. Level-3 daily data for 0.25° by 0.25° grid cells for 2010-2019 were also acquired from the Giovanni website for O&G and Urban NO_2 zones. The O&G zone has southwest coordinates of 40°N and 105.25°W and northeast coordinates of 40.75°N and 104.5°W. The Urban zone has southwest coordinates of 39.5°N and 105.25°W and northeast coordinates of 40°N and 104.75°W. Annual averages were computed from daily data, and only values above zero were retained. Annual OMI NO_2 were used to

represent NO_x and to test for its effects on O_3. The OMI NO_2 data are described by Krotkov et al. (2019) and Krotkov et al. (2017). Satellite overflights occur ~13:30 LST. Annual average surface concentrations for NO_2 were also acquired from CDPHE and the EPA for CAMP (at 1,593 m MSL and 39.75° N, 104.99°W) and Welby (at 1,554 m MSL and 39.84°N, 104.95°W) to compare with OMI NO_2 and verify percent changes in NO_2 from 2012-2019. Site locations are shown in Figure 3.

Monitor footprints showing relative spatial contributions of areas upwind at FTCW, WCT, RFLAT, and CHAT were developed using NOAA hybrid single-particle Lagrangian integrated trajectory (HYSPLIT) back trajectories (Rolph et al., 2017; Stein et al., 2015) and generated online with EDAS 40 km meteorology (arrival heights of 100 m), using a methodology outlined by Reddy and Pfister (2016). Footprints are based on the densities of 24-hour back trajectory points for each hour contributing to the maximum 8-hour concentrations for the four highest days in 2016 and 2017 (after removal of days flagged for possible influences from smoke or stratospheric intrusions). Point counts were calculated and contoured for 0.1° by 0.1° cells.

2.2 Bayesian Correlation Analysis

This assessment of the effects of O&G VOC emissions reductions on O_3 relies heavily on correlation analyses. Within the classic or "frequentist" framework of correlation analysis, the strength and significance of a correlation are tested with the correlation coefficient and *p*, and a correlation is considered statistically significant if *p* is ≤ 0.05. The *p* value does not yield information about the probability that the study hypothesis is true. It simply represents the probability of finding a correlation value at least as extreme in random sampling of data where the true correlation is zero (Nuzzo, 2017). In addition, classic correlation does not provide an estimate of the probability that a study hypothesis is true (Nuzzo, 2017). It is also possible to have a high correlation and low *p* that misrepresent the actual strength of the evidence. See, for example the correlation of 0.73 between NREL annual fourth maximum 8-hour O_3 and Platteville ethane in Table 1 in Section 3.4. Based on Bayesian methods, this correlation has a relatively low probability of proving an interrelationship between these two variables since the probability is only 2.6 times higher than the null hypothesis. To address this potential insufficiency in standard null hypothesis significance testing, I generated Bayesian correlation factors using the JASP open-source software package (Kelter, 2020; Nuzzo, 2017). These factors provide a robust statistical measure of the strength of the evidence supporting the study hypotheses and give the investigator much more information than the Pearson correlation and *p* to choose between potentially competing hypotheses (Kass and Raftery, 1995).

The Pearson correlation coefficients in classic and Bayesian analyses are identical. The strength of the evidence under Bayesian analysis, however, is represented by the Bayesian correlation factor BF_{10} (Kelter, 2020; Ruiz-Ruano García and López Puga, 2018; Nuzzo, 2017) or the Vovk-Sellke maximum p-ratio (VS-MPR) (Sellke et al., 2001). These metrics provide an indication of how much more likely the study hypothesis is than the null hypothesis. The use of VS-MPR leads to more accurate decisions about hypotheses than *p* alone, and BF_{10} is more accurate than VS-MPR (Ruiz-Ruano García and López Puga, 2018). VS-MPR is an indicator of the maximum possible odds or the upper bound of the Bayes factor. A BF_{10} of 0.33 to 1.00 is considered anecdotal evidence that the null hypothesis is true. A BF_{10} of 1 to 3 signifies anecdotal evidence in support of the study hypothesis, 3 to 10 signifies substantial evidence, 10 to 30 strong

evidence, 30 to 100 very strong evidence, and higher than 100 signifies decisive evidence (Ruiz-Ruano García and López Puga, 2018; Kelter, 2020). Partial correlations and partial regressions were also used in this study to isolate the impacts of VOCs (as represented by ethane) and NO_x (as represented by OMI NO_2). JASP generates VS-MPR values for partial correlations.

Bayesian analysis considers prior and posterior knowledge about the relationships between variables and allows the investigator to factor in prior knowledge of possible interrelationships and effects based on the results of previous research. Patterns and effects identified in a current analysis of variable pairs cannot be considered prior knowledge. The default setting in JASP is that there is no prior information about the interrelationships considered. In this case, under the prior condition, any correlation coefficient between -1 and 1 is considered equally likely (Nuzzo, 2017). Using information from previous research studies, it is possible to set as prior conditions the knowledge that correlations will be either all positive or all negative. The default setting is used in this study, unless otherwise stated.

3 Results and Discussion

3.1. Relationships between AIRS DDJB Methane Enhancements, Platteville Ethane, and Ozone SIP Oil and Gas VOC Emissions

There is a surprising consistency between trends in O_3 SIP O&G VOC emissions, Platteville median ethane, and the AIRS satellite-derived methane enhancement for the entire DDJB. Figure 1 below shows linear regressions for SIP O&G VOC emissions (2011-2020) and Platteville median ethane (2012-2020) versus DDJB methane enhancement. The R^2 values are 0.77 for emissions and 0.93 for ethane. Each intercepts the x-axis (at zero emissions and ethane) at a DDJB methane enhancement value that is ~30% of 2012 methane. This is consistent with the estimate of 25% for non-O&G methane in the area in 2012 (Petron et al., 2014). O&G activities are the predominant source for ethane in the region (as reported in the literature and summarized by Reddy and Taylor, 2022). Trends in the emissions inventory provide evidence for the cause of trends in both ethane and methane. The BF_{10} is 44 for emissions versus methane enhancement and 146 for emissions versus ethane. This means that these interrelationships are 44 and 146 times more likely, with strong and decisive evidence, respectively, than no connection at all. The correlation between DDJB methane enhancement and Platteville median ethane is 0.96 (Reddy and Taylor, 2022), and this has a BF_{10} of 465. This increases to 931 if we factor in the prior knowledge that ethane and methane in the DM/NFR are primarily from O&G sources and must be positively correlated. This signifies decisive evidence for a linear connection between the two. It is reasonable to use Platteville ethane as a tracer for O&G VOCs.

3.2 Monitor Footprints Based on HYSPLIT

Monitor footprints were calculated for FTCW, WCT, RFLAT, and CHAT using HYSPLIT back trajectory point counts for 24-hour back trajectories for each hour contributing to the maximum 8-hour concentrations for the four highest days in 2016 and 2017. Trajectory point counts were calculated from aggregated HYSPLIT output data for 0.1° by 0.1° cells and then contoured. Counts above 10 per cell are shown in Figure 2. Both FTCW and WCT have strong influences from the O&G fields on maximum concentration days. RFLAT has both O&G and urban area influences. The CHAT source area is primary urban in nature. FTCW, RFLAT, and CHAT show

the influences of summer daytime thermally-driven upslope flow towards higher terrain (as described by Toth and Johnson, 1985), and this flow regime is associated with high O_3 events (Flocke et al., 2020; Pfister and Reddy et al. 2017; Reddy and Pfister, 2016). The FTCW, RFLAT, and CHAT footprints are nearly identical to those calculated for 2006-2008 by Reddy and Pfister (2016).

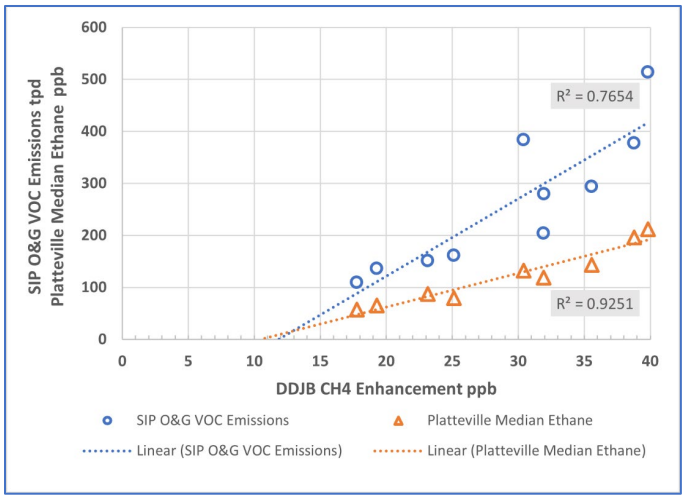

Figure 1. Linear regressions for O&G VOC emissions estimates (2011-2020) and Platteville median ethane (2012-2020) versus AIRS satellite-derived DDJB methane enhancement.

Pfister et al. (2019) indicate that their 2014 FRAPPÉ O&G photochemistry study area which includes the Wattenburg Field east of BAO and the Greeley area has the highest net O_3 production rates in the DM/NFR. Higher VOC emissions here lead to a higher abundance of peroxyl radicals which ultimately lead to NO_2, and this can be photolyzed to create O_3. The monitor footprints show that this area is a significant source region for maximum O_3 concentration events at FTCW, WCT, and RFLAT. Pfister and Flocke et al. (2017) and Pfister et al. (2019) also conclude that the O&G area and Fort Collins are closer to being NO_x sensitive for O_3, while the City study area which includes CHAT and NREL is closer to being VOC sensitive.

3.3 Local OMI Tropospheric NO_2

Annual average column OMI tropospheric NO_2 for the study area is shown for 2012 and 2019 in Figure 3. NO_2 in molecules per cm^2 has been gridded into 0.25° by 0.25° cells by NASA. Figure 4 shows the percent change in each grid from 2012 to 2019. These are decreases in all cases. OMI NO_2 shows a 29% decrease in the cell where the CDPHE CAMP and Welby monitors are located. Annual average NO_2 measured at the CAMP monitor decreased 24% during this period, and at the Welby monitor NO_2 decreased by 12%, based on simple differences from 2012-2019.

The footprint outlines for FTCW and CHAT were used to specify an O&G region and an Urban region, respectively, for OMI NO_2. These regions are outlined in green in Figure 4b. Annual average OMI tropospheric NO_2 for 2010-2019 for these zones was used in the correlation and regression analyses discussed in Section 3.4. The Pearson correlation between OMI tropospheric NO_2 for the Urban region and annual NO_2 at CAMP for 2012-2019 is 0.88 with a BF_{10} of 12.7, showing good agreement between the two and strong evidence that Urban zone OMI NO_2 tracks

with NO_2 in downtown Denver during the period used to evaluate the sensitivity of O_3 to both ethane and NO_2. This is comparable to correlations of 0.68-0.86 found for OMI NO_2 and surface NO_2 at urban sites in major European cities (Paraschiv et al., 2017). Comparisons of FRAPPÉ and DISCOVER-AQ aircraft measurements of NO_2 and OMI tropospheric NO_2 for the DM/NFR region during July-August 2014 showed correlations of 0.7 but a low bias of ~40% in the OMI product (Choi et al, 2020). There were no continuous surface NO_2 measurements for 2012-2019 in the O&G zone.

Linear regressions between annual OMI NO_2 and year from 2010-2019 show an 11% reduction for the O&G region and a 22% reduction for the Urban region between 2012 and 2019. Regression statistics and plots for OMI NO_2 versus year for the O&G and Urban NO_2 regions in Figure 4b are described and presented in Figure S1 and accompanying text. OMI NO_2 reductions for the Urban region are generally consistent with reductions at CAMP, and these are much less than the 67% decrease in Platteville ethane (based on simple differences between 2012 and 2019 values) for the same period.

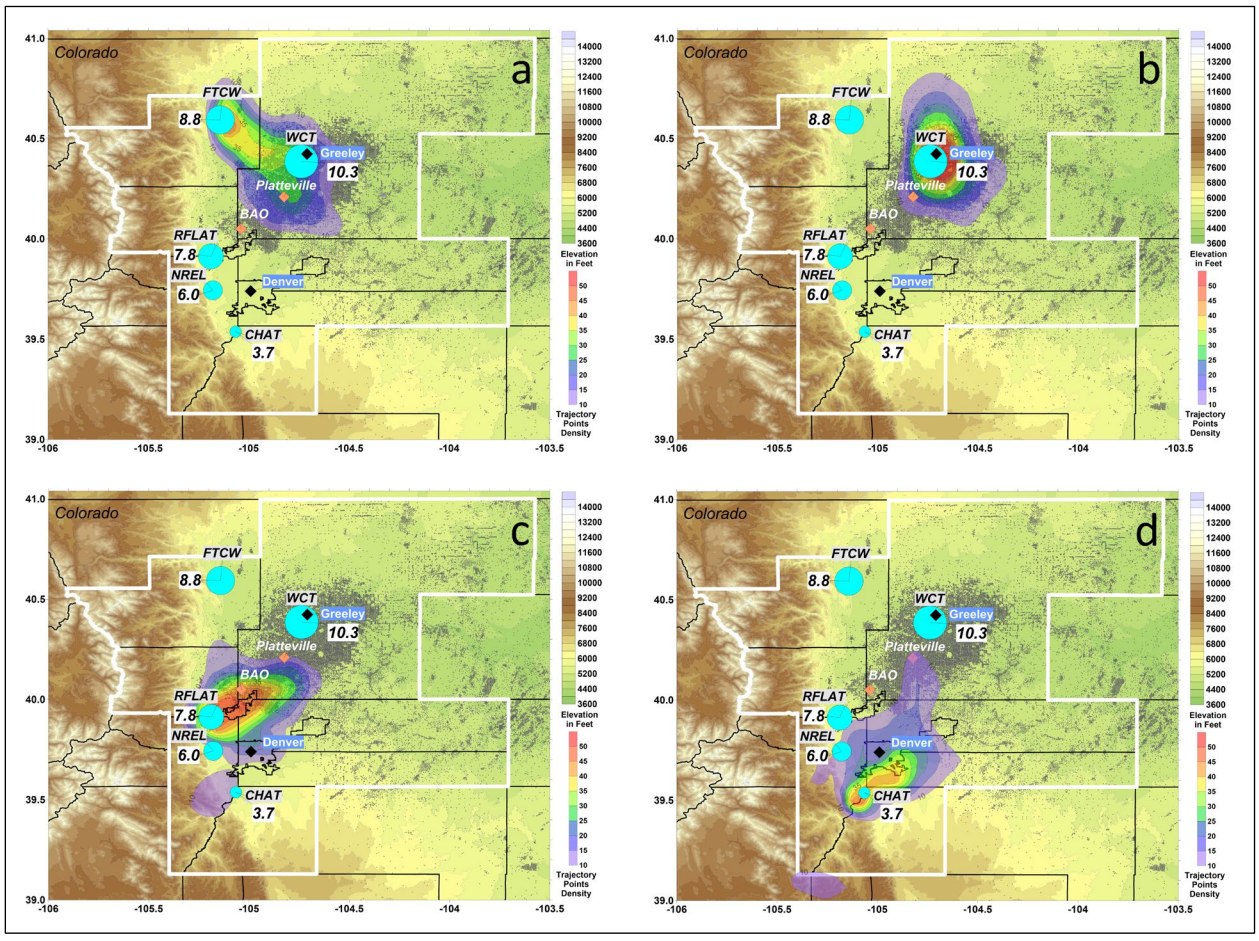

Figure 2. Monitor footprints for (a) FTCW, (b), WCT, (c) RFLAT, and (d) CHAT showing contours of back trajectory point counts the for 24-hour back trajectories for each hour contributing to the maximum 8-hour concentrations for the four highest days in 2016 and 2017. Trajectory point counts were calculated from aggregated HYSPLIT output data for 0.1° by 0.1° cells and then contoured. Counts above 10 per cell are shown. The differences

between 2012 and 2019 fourth maximum 8-hour O_3 in ppb (scaled blue circles) for FTCW, WCT, RFLAT, NREL, and CHAT are also plotted. O_3 differences are reductions. O&G wells are shown as gray dots, and the O_3 NAA is outlined in white.

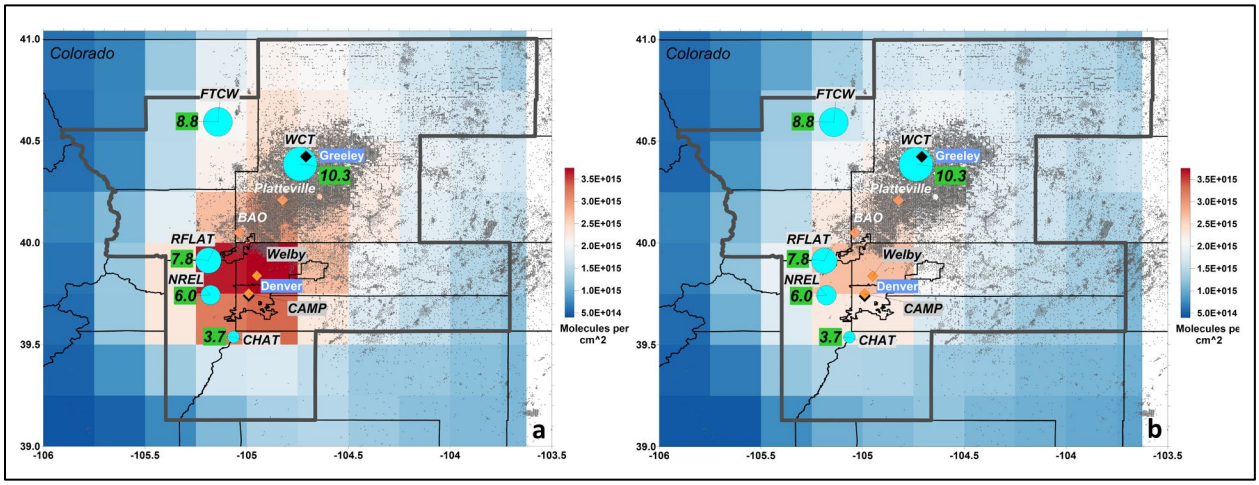

Figure 3. Annual mean OMI tropospheric NO_2 in molecules per cm^2 gridded into 0.25° by 0.25° cells for (a) 2012 and (b) 2019 (colored tiles) and differences between 2012 and 2019 fourth maximum 8-hour O_3 in ppb (from Table 1, scaled blue circles) for FTCW, WCT, RFLAT, NREL, and CHAT. O_3 differences are reductions. O&G wells are shown as gray dots, and the O_3 NAA is outlined in black.

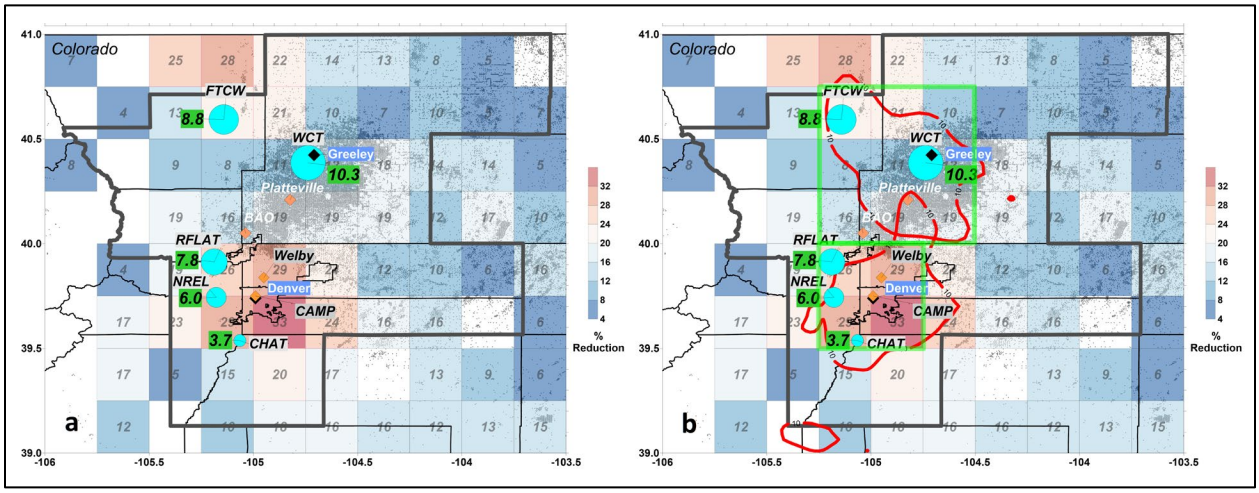

Figure 4. (a) Percent reductions in gridded annual mean OMI tropospheric NO_2 between 2012 and 2019 (colored tiles) and differences between 2012 and 2019 fourth maximum 8-hour O_3 in ppb (from Table 1, scaled blue circles) for FTCW, WCT, RFLAT, NREL, and CHAT. O_3 differences are reductions. (b) The same as (a) with outlines of monitor footprints for FTCW and CHAT (in red) and associated OMI tropospheric NO_2 footprint region squares (in green) for the O&G region (north) and Urban region (south). O&G wells are shown as gray dots, and the O_3 NAA is outlined in black.

3.4. Bayesian Correlation Analyses of Relationships between Annual Fourth Maximum 8-hour O_3 at Key Sites and Platteville Ethane, SIP O&G VOC Emissions, DDJB Methane Enhancements, OMI Tropospheric NO_2, and Modeled Source Contributions to O_3.

Key correlations, the 2017 modeled source contributions at five monitors, and changes in annual fourth maximum 8-hour O_3 at these sites are presented in Table 1. The modeled O&G contributions include the effects of both VOCs and NO_x. McDuffie et al. (2017) report that total O&G emissions typically contributed 3.1 ppb of O_3 at the BAO within the O&G field in 2012 compared to 2.9 ppb with only O&G VOC emissions, so it is reasonable to assume that most of the modeled O&G contributions are due to VOCs. The OR, NR, and EGU sources listed in column 8 are the major sources for NO_x emissions. Linear regressions between annual fourth maximum 8-hour O_3 versus year for 2011-2019 were used to compute the declines in the last two columns of Table 1 and are plotted and described in Figure S2 and associated text.

In Table 1, correlations that provide strong to decisive evidence of an effect on O_3 are highlighted in orange. Those that provide substantial evidence based on BF_{10} are highlighted in green. Those that provide anecdotal evidence are shaded in gray, and those that show anecdotal evidence for the null hypothesis are highlighted in pink. The sample numbers (n) in Table 1 reflect the removal of outliers having studentized residuals greater than or equal to 2.5 as determined by regressing O_3 against ethane. Outliers were not found in regressions with NO_2. In all cases, fourth maximum concentrations were determined after events flagged for possible influences from wildfire smoke or stratospheric intrusions had been removed.

FTCW and RFLAT O_3 stand out as highly correlated with Platteville median ethane, the SIP O&G VOC emissions, AIRS DDJB methane enhancements, and annual mean OMI tropospheric NO_2 for the O&G region (see Figure 4b). Plots of regressions against ethane and NO_2 for these sites are presented in Figures 5 and 6, respectively. Correlations at FTCW and RFLAT also have high values for BF_{10} or VS-MPR in most instances. The BF_{10} factor of 483 shows that the 0.99 correlation between FTCW O_3 and Platteville ethane is decisive, proving that O_3 here has a direct linear connection with ethane, a tracer for O&G VOC emissions. An interconnection is 483 times more likely than no interconnection at all, and it signifies a direct response. Without the removal of days flagged for possible smoke or intrusion influences, the correlation and BF_{10} for FTCW are only 0.91 and 12, respectively. Given our knowledge from previous work about the scale of the reductions in O&G VOC emissions (Reddy and Taylor, 2022) and the effects that a zero-out scenario would have on O_3 (Pfister and Flocke et al., 2017), it is reasonable to assume that FTCW and RFLAT O_3 would be positively correlated with ethane. Setting this as a prior condition leads to a BF_{10} of 966 and 83 for FTCW and RFLAT, respectively.

The correlation between FTCW O_3 and OMI NO_2 for the O&G region is 0.89 with a BF_{10} of 17. It is likely that this high correlation is at least partially due to phased regulatory controls of VOCs (see Reddy and Taylor, 2022) and simultaneous NO_x emissions reductions. The eigenvalue of uncentered correlations from a linear regression against both ethane and NO_2 suggests that collinearity is a problem (eigenvalue of 5,718), and this could be explained by independent reductions in each that track together. The likelihood of a response to ethane, however, is 28 times greater (BF_{10} ratio = 483/17) than the likelihood of a response to NO_2.

Table 1. Pearson Correlations between Annual Fourth Maximum 8-hour O_3, Platteville Median Ethane, O_3 SIP O&G VOC Emissions, and DDJB Methane Enhancement for 2012-2019 for 5 Key Sites; Partial Pearson Correlations between Annual Fourth Maximum O_3 and Platteville Median Ethane for 2012-2019 Conditioned for OMI Tropospheric NO_2; 2017 NAA Average Modeled O&G and Total OR, NR, and EGU Contributions to the 10 Highest Modeled 8-hour O_3; and Differences between 2012 and 2019 and 2014 and 2019 Fourth Maximum O_3 Based on 2011-2019 Regressions between O_3 and Year.

	Correlations with Fourth Max 8-hour O_3 2012-2019								
Sites from North-South	Platteville Median Ethane	O_3 SIP O&G VOC Emissions	AIRS DDJB Methane Enhancement	Partial Correlations with Platteville Ethane, Conditioned for OMI NO_2	Annual Mean OMI Tropospheric NO_2	Average of Top 10 Days: 2017 O&G Contribution to O_3	Average of Top 10 Days: 2017 OR, NR, and EGU Contribution to O_3	2012 minus 2019 Fourth Max O_3 from 2011-2019 Regressions	2014 minus 2019 Fourth Max O_3 from 2011-2019 Regressions
FTCW	**0.99** n=7 P<0.001 BF_{10}=483.1	**0.88** n=7 P=0.009 BF_{10}=7.4	**0.96** n=7 P<0.001 BF_{10}=38.5	**0.96** n=7 P=0.003 VS-MPR=22.8	**0.89** n=8 P=0.003 BF_{10}=17.3	6.6 ppb	7.5 ppb	8.8 ppb	6.3 ppb
WCT	**0.93** n=6 P=0.007 BF_{10}=8.4	**0.86** n=6 P=0.030 BF_{10}=3.3	**0.86** n=6 P=0.030 BF_{10}=3.3	**0.58*** n=6 P=0.307 VS-MPR=1.0	**0.75** n=8 P=0.034 BF_{10}=3.0	7.0 ppb	5.0 ppb	10.3 ppb	7.4 ppb
RFLAT	**0.96** n=7 P<0.001 BF_{10}=41.6	**0.94** n=7 P=0.002 BF_{10}=24.5	**0.93** n=7 P=0.003 BF_{10}=16.7	**0.87** n=7 P=0.026 VS-MPR=3.9	**0.79** n=8 P=0.019 BF_{10}=4.4	3.5 ppb	9.0 ppb	7.8 ppb	5.6 ppb
NREL	**0.73** n=8 P=0.041 BF_{10}=2.6	**0.66*** n=8 P=0.077 BF_{10}=1.7	**0.79** n=8 P=0.020 BF_{10}=4.4	**0.82** n=8 P=0.024 VS-MPR=4.1	**0.50*** n=8 P=0.210 BF_{10}=0.9	2.9 ppb	8.8 ppb	6.0 ppb	4.3 ppb
CHAT	**0.60*** n=8 P=0.113 BF_{10}=1.3	**0.50*** n=8 P=0.203 BF_{10}=0.9	**0.51*** n=8 P=0.196 BF_{10}=0.9	**0.63*** n=8 P=0.130 VS-MPR=1.4	**0.42*** n=8 P=0.299 BF_{10}=0.7	1.7 ppb	9.6 ppb	3.7 ppb	2.7 ppb
*Not statistically significant									

Partial correlations were also calculated for O_3 versus ethane and presented in Table 1. These partial correlations remove the influences of NO_x as represented by OMI tropospheric NO_2 and can be effective provided a linear response to NO_x is a reasonable approximation. The partial correlation between FTCW O_3 and ethane is 0.96 with a strong VS-MPR of 22.8. It also shows a direct connection between O_3 and O&G VOCs.

The influence of meteorology was not included in a partial correlation analyses. From 2012-2019, meteorology as represented by June-August mean 500 hPa heights, had an indeterminant effect on O_3 screened for flagged events. This is likely due to the dominant effects of emissions reductions during the period. The *p* values for correlations between O_3 and 500 hPa heights at all sites were 0.159-0.315 and BF_{10} values were 0.5-0.6 for all sites, showing anecdotal support for the null hypothesis.

In contrast to partial correlations with ethane conditioned for OMI NO_2, partial correlations between annual fourth maximum O_3 and OMI NO_2 conditioned for ethane were statistically insignificant at every site with *p* values from 0.086 to 0.786 and VS-MPR from 1.0 to 1.7. At FTCW the partial correlation was 0.14 (*p* of 0.786, VS-MPR of 1.0). For FTCW in particular, this is compelling evidence that most of the decrease in O_3 from 2012 to 2019 may be the result of reductions in O&G VOCs and not NO_x, despite the high standard correlation of 0.89 with NO_2. JASP partial regression plots show a strong response to ethane in Figure 7a and a weak response to NO_2 in Figure 7b. Residuals of FTCW O_3 regressed against NO_2 versus the residuals from ethane regressed against NO_2 are plotted in Figure 7a, and residuals of FTCW O_3 regressed

against ethane versus residuals of NO_2 regressed against ethane are shown in Figure 7b.

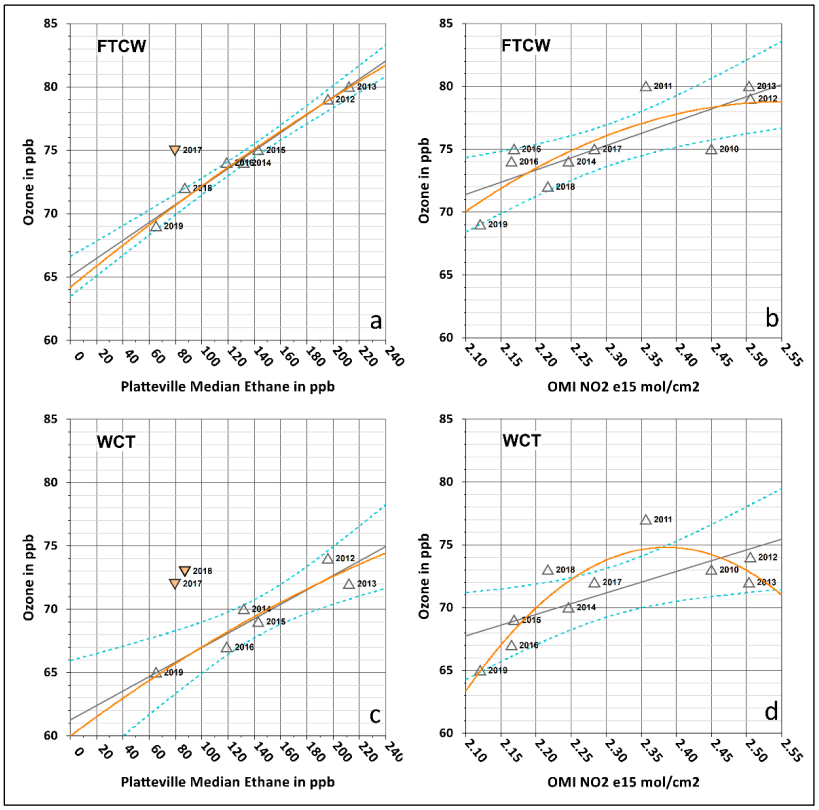

Figure 5. Annual fourth maximum 8-hour O_3 (determined after removal of events flagged for possible influences from wildfire smoke or stratospheric intrusions) versus annual Platteville median ethane with linear regressions and 95% confidence limits (dotted blue lines) for (a) FTCW and (c) WCT from 2012-2019 and versus OMI tropospheric NO_2 for (b) FTCW and (d) WCT for 2010-2019. Fitted second order polynomial curves are shown in orange, and outliers that were removed prior to regressions based on studentized residual tests are shown with inverted triangles. FTCW and WCT tropospheric OMI NO_2 were calculated for the O&G region (as shown in Figure 4b).

The partial R^2 for FTCW O_3 versus ethane conditioned for NO_2 at this site is 0.92, suggesting that ~90% of the variance in O_3 here is due to changes in O&G VOCs as represented by ethane (75% at RFLAT). It is reasonable to conclude that a substantial and perhaps dominant fraction of the O_3 decrease here is due to O&G VOC reductions. The ~9 ppb decline in O_3 at FTCW from 2012-2019 is in the range of the estimated contribution to O_3 by O&G VOCs at this site on maximum concentration days from 2012 through 2017 as reported in the literature and discussed in Section 1. A considerable reduction in O_3 is consistent with the ~70% reduction in O&G emissions from 2013-2020 inferred by Reddy and Taylor (2022). Similar linear responses of O_3 to VOCs are difficult to find in the literature, although Barna et al. (2011) report linear responses to VOCs downwind of Seattle and Portland based on modeling of the Cascadia airshed.

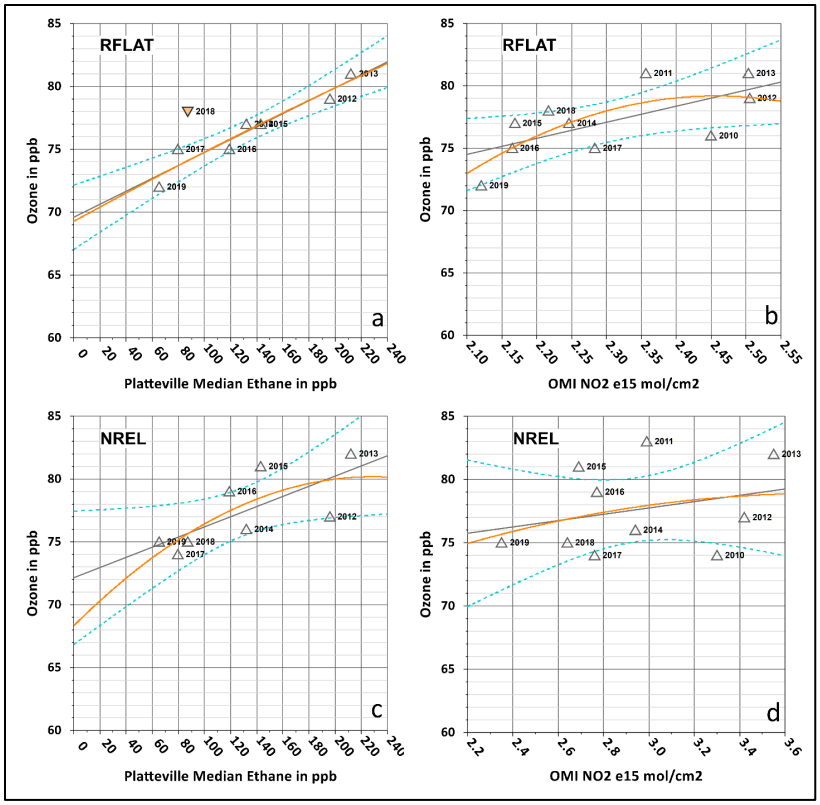

Figure 6. Annual fourth maximum 8-hour O_3 (determined after removal of events flagged for possible influences from wildfire smoke or stratospheric intrusions) versus annual Platteville median ethane with linear regressions and 95% confidence limits (dotted blue lines) for (a) RFLAT and (c) NREL from 2012-2019 and versus OMI tropospheric NO_2 for (b) RFLAT and (d) NREL for 2010-2019. Fitted second order polynomial curves are shown in orange, and an outlier based on studentized residual tests that was removed prior to regression is shown with an inverted triangle in (a). RFLAT tropospheric OMI NO_2 was calculated for the O&G region and NREL OMI NO_2 was calculated for the Urban region (as shown in Figure 4b).

The WCT tower on the southern edge of Greeley is unique among the 5 sites considered. It is the only neighborhood scale monitor of the group. The others are in open fields or a park and are not as directly affected by neighborhood emissions of fresh NO and NO_x from mobile sources. In the report by Pfister and Flocke et al. (2017) detailing the findings of the 2014 FRAPPÉ field experiment for CDPHE, the WCT site is described as starved for NO_x and most sensitive to NO_x reductions, with O_3 production peaking earlier in the day than at locations downwind. WCT which is at the bottom of the broad Platte River Valley is also in a portion of the DM/NFR with the slowest growth in daytime boundary layer heights (Pfister et al., 2019), and this means that precursors are more concentrated here during the early hours of O_3 production.

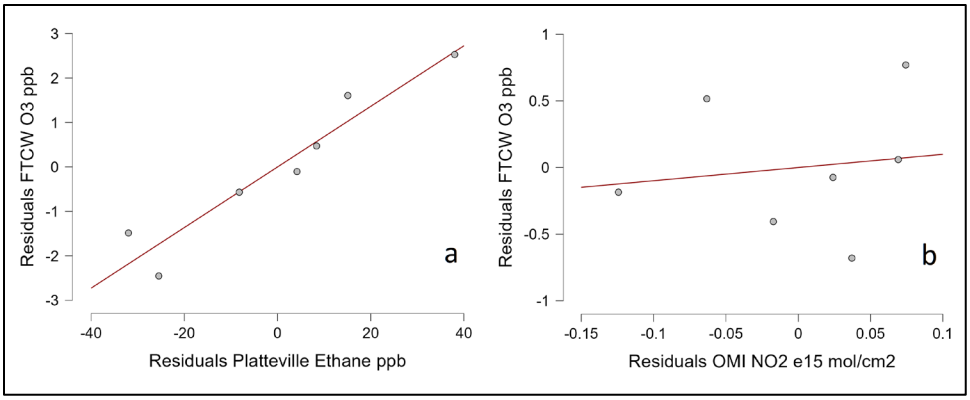

Figure 7. Partial regression plots of (a) residuals of FTCW O_3 versus OMI NO_2 (y axis) and ethane versus OMI NO_2 (x axis) and (b) residuals of FTCW O_3 versus ethane (y axis) and OMI NO_2 versus ethane (x axis), showing a strong response to (a) ethane and weak response to (b) NO_2.

Figure 5 shows plots of FTCW and WCT O_3 versus ethane and OMI tropospheric NO_2 calculated for the O&G region). The plot of WCT O_3 versus NO_2 shows a curved response and a second order polynomial is a better fit than a linear regression. The curve suggests that WCT may have been NO_x-saturated prior to 2014 with a flat or increasing O_3 response to NO_2 reductions during this period. After 2013, O_3 declines steeply with decreasing NO_2. Correlations between WCT O_3 and ethane and NO_2 (BF_{10} of 8.4 and 3.0, respectively) are weaker here than at FTCW and RFLAT. The partial correlations of O_3 versus ethane conditioned for NO_2 and NO_2 conditioned for ethane are both statistically insignificant. Changes in both precursor groups and other factors may contribute significantly to the 10 ppb decrease in O_3 here from 2012-2019. This relative complexity compared to FTCW, the lower sample size for O_3 versus ethane after outlier removal, and significantly non-linear response to NO_2 may make it more difficult to identify a dominant cause for O_3 decreases.

Figure 6 shows O_3 versus ethane and OMI tropospheric NO_2 for RFLAT and NREL. NO_2 for RFLAT was calculated using the O&G region, and the Urban region was used for NREL. RLAT O_3 has a robust response to ethane and declines with NO_2 as well. NREL has a statistically significant response to ethane but not to NO_2, and the uncertainties for regressions against each precursor are greater than for RFLAT which is further north.

For CHAT, correlations show at best only anecdotal evidence of the study hypothesis or anecdotal evidence for the null hypothesis (BF_{10} between 0.33 and 1.4). In addition, the slope of the 2011-2019 regression of annual fourth max versus year and slopes for both regressions in Figure 8 are not statistically significant. Since evidence for a response to ethane or NO_2 is weak and the variances in O_3 are high, it is possible that factors affecting the photochemical regime here are more complex than at FTCW and that as of 2019 there have not been sufficient reductions in either VOCs or NO_x to shift the regime to one that is substantially sensitive to reductions in either or both of these precursor groups. In addition, reductions in urban VOCs have not been considered.

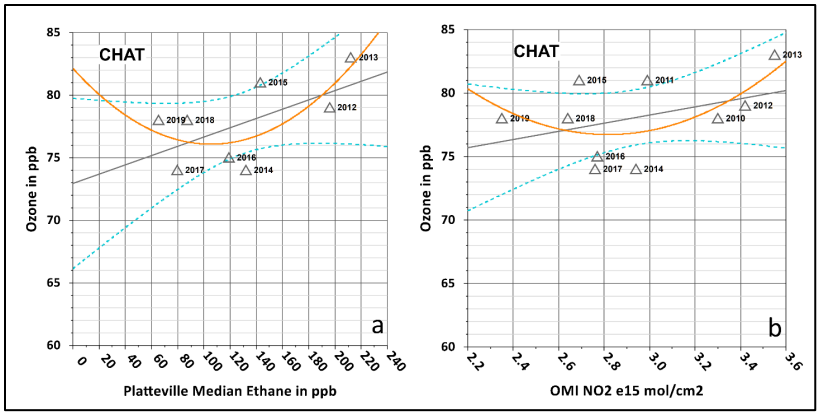

Figure 8. Annual CHAT fourth maximum 8-hour O_3 (determined after removal of events flagged for possible influences from wildfire smoke or stratospheric intrusions) versus (a) annual Platteville median ethane with linear regressions and 95% confidence limits (dotted blue lines) and (b) versus annual mean OMI tropospheric NO_2. Fitted second order polynomial curves are shown in orange. Annual CHAT tropospheric OMI NO_2 was calculated for the Urban region (as shown in Figure 4b).

Modeled O&G source contributions to O_3 and decreases in annual fourth maximum O_3 during the study period show a pronounced decreasing gradient from FTCW and WCT to Chatfield. This is consistent with the findings of Flocke et al. (2020) and Pfister and Flocke et al. (2017) who report that O&G influences are higher in the northern portions of the region. The 2017 O&G contributions to O_3 in Table 1 are also highly correlated with the differences in annual fourth maximum concentrations between 2014 and 2019 from Table 1. The Pearson correlation is 0.93 (BF_{10}=4.0). The regression between the 2014-2019 decreases in O_3 and 2017 O&G contributions is presented in Figure 9a, and it has an R^2 value of 0.87 (VS-MPR=4.6). Figure 9b shows a reverse gradient for 2017 NO_x source contributions versus O&G contributions. Greater decreases in O_3 to the north match the greater influence of O&G emissions here, and the scale of decreases is consistent with a large decline in O&G emissions. The fact that correlations metrics in Table 1 also conform to this gradient is further evidence that substantial reductions in O&G VOC emissions have affected maximum O_3. A summary map illustrating the north-south gradients in correlation metrics and impacts is presented in Figure 10.

This analysis is entirely empirical and does not explicitly address complex nonlinear photochemical interactions and processes, and it does not account for the possible implications of the effects of changing chemical environments on trends in NO_2 (Laughner and Cohen, 2019). Nevertheless, it points to a strong linear response in O_3 to decreasing VOCs during the study period (especially at FTCW and RFLAT) and possible nonlinear responses to changes in NO_x, especially at WCT. The strong statistical results at the northern monitors are consistent with what we know from photochemical modeling and what monitor footprints show us about source influences. These results are believed to be sufficient evidence for the inferences made here. Interrelationships among emissions estimates, satellite-derived methane enhancements, ethane, and maximum O_3 concentrations provide coherent evidence for major reductions in local O&G VOC emissions and related decreases in O_3.

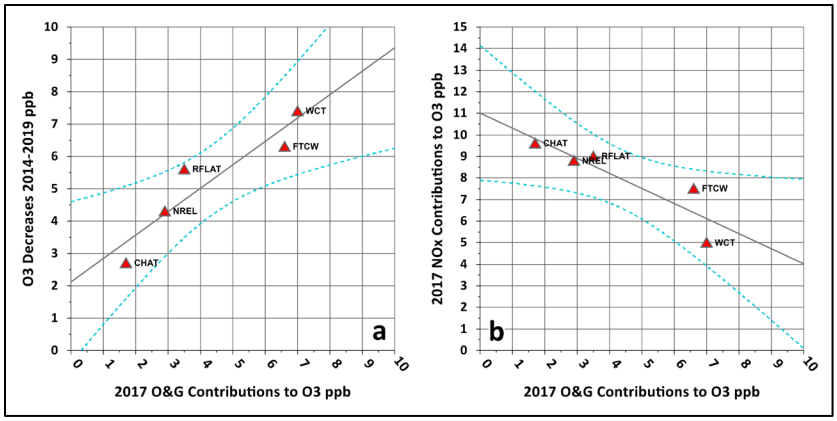

Figure 9. (a) Linear regression between the decreases in O_3 from 2014-2019 and modeled 2017 O&G contributions to O_3 by monitor site (R^2 of 0.87 and VS-MPR of 4.6). The 95% confidence limits are plotted as dashed lines. There is a north-south gradient in decreases in O_3 associated with decreases in O&G VOC. (b) 2017 NO_x sources contributions to O_3 (OR, NR, and EGU sources) versus O&G contributions to O_3, showing a reverse gradient.

Platteville median ethane and SIP O&G VOC emissions declined by 67% and 64%, respectively, between 2012 and 2019 (based on simple differences between 2012 and 2019 values). Given the linear decline in O_3 with respect to ethane at FTCW and RFLAT and robust correlation metrics at these sites for variables related to O&G VOC emissions, it is possible that as much as 67% of the O_3 from O&G VOCs at these sites was eliminated between 2012 and 2019. The impacts of trends in background O_3 from outside the DM/NFR were not considered and are beyond the scope of this study, but these are not expected to have significant effects on the results. The change in FTCW O_3 from 2012-2019, for example, is ~9 ppb whether it is derived from the regression of O_3 versus time or O_3 versus Platteville ethane.

Zeroing-out ethane (and by extension, O&G VOC emissions) in the regressions shown in Figures 5-6 yields annual fourth maximum O_3 of 65 ppb (±1.6 ppb) at FTCW, 61 ppb (±4.7 ppb) at WCT, and 70 ppb (± 2.6 ppb) at RFLAT. Uncertainties represent the 95% confidence interval. These concentrations could keep FTCW and WCT in compliance with the 2015 NAAQS and RFLAT within reach of compliance, provided that emissions from other sources did not increase, climate conditions do not favor enhanced photochemistry, and frequent periods of wildfire smoke did not elevate local and background O_3.

These zero-out projections are most appropriate for FTCW and RFLAT where correlations are highest, a linear fit is a reasonable approximation of the response of O_3 to NO_2, and the partial correlations and partial regressions are most likely to reasonably separate the influences of O&G VOCs and NO_x. Partial regressions of O_3 versus ethane at these sites using natural-log-transformed OMI NO_2 to correct for nonlinearity yield partial R^2 values of 0.92 and 0.76 at FTCW and RFLAT, respectively. These are essentially identical to the partial R^2 values under the assumption that responses to NO_2 are effectively linear, and continue to confirm that VOCs have much larger contributions to O_3. At WCT the partial R^2 values using log-transformed NO_2 are 0.32 and 0.19 for ethane and NO_2, respectively, compared to 0.33 and 0.18 assuming linear relationships in each case. Again, the WCT data suffer from a lower sample size and possibly a

noisier signal. Previous research as well as the research presented here, however, suggest that this site should benefit from both O&G VOC and NO_x reductions.

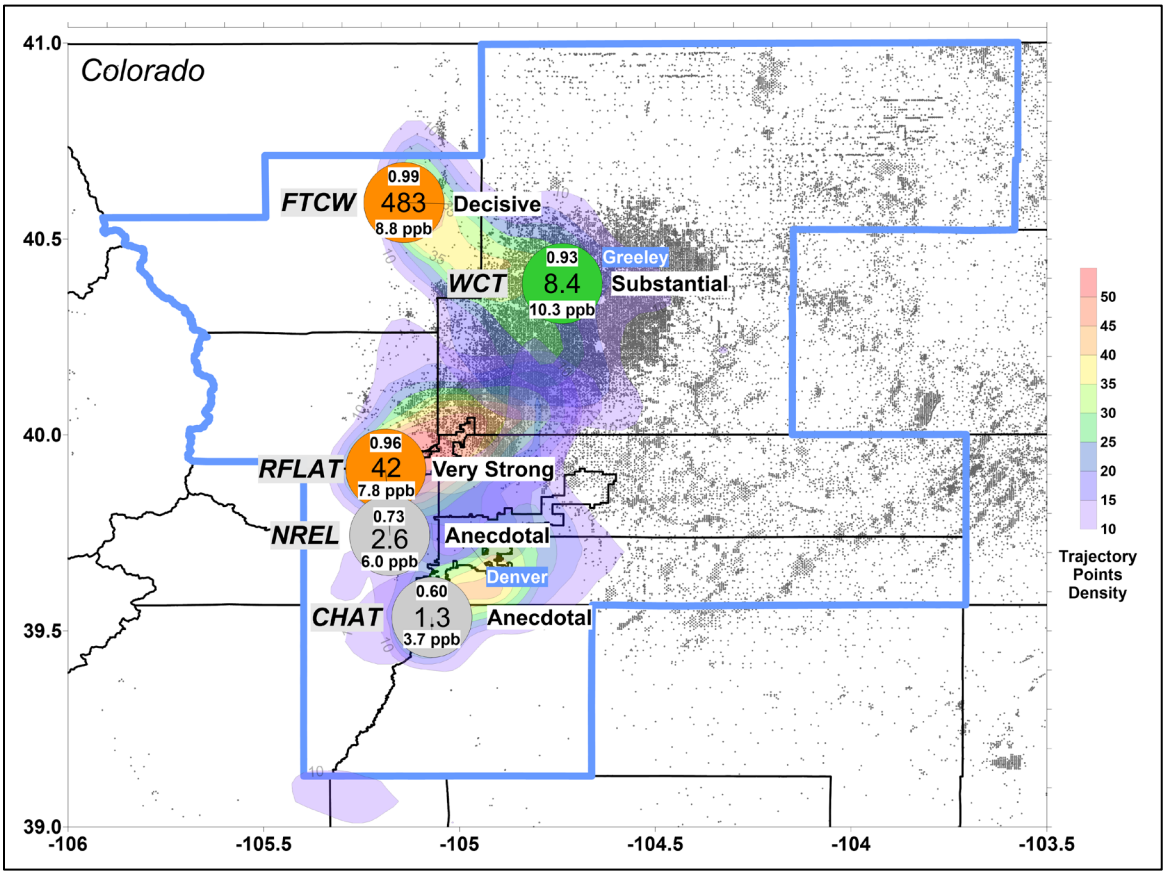

Figure 10. O_3 correlations with Platteville ethane, Bayesian correlation factor (BF_{10}) values for O_3 and ethane, and O_3 decreases from 2012-2019 (from top to bottom in each circle) are presented for the five high-concentration sites. The monitor site circle colors gray, green, or orange represent Bayesian indications of anecdotal, substantial, or very strong/decisive evidence of an interconnection, respectively. Monitor footprints for FTCW, RFLAT, and CHAT are plotted. O&G wells are represented by gray dots, and the NAA is outlined in blue. The influences of the O&G field, O_3 impacts from decreased O&G VOC emissions, and correlation metrics decrease from north to south.

3.5 Top-down Methane Flux Studies from 2012 to 2021 and Their Implications for Tracking O&G Emissions

Tracking trends in methane and methane emissions in the DM/NFR makes it possible to assess progress in reducing O_3 and achieving greenhouse gas reduction goals (Colorado Department of Public Health and Environment, 2021). A number of top-down methane flux studies have been completed for the DM/NFR region. These include flux estimates based on two NOAA flights in late May 2012 (Petron et al., 2014), two NOAA flights in March 2015 (Peischl et al., 2018), two University of Colorado (CU) and University of Maryland (UMD) flights in early October 2021 (Fried et al., 2022), a driving survey in the summer of 2021 (Riddick et al., 2022), and a

University of Arizona satellite methane inversion analysis for June-July and September-October 2021 (Cusworth et al., 2022). The inversions used column-average methane concentrations retrieved from the TROPOspheric Monitoring Instrument (TROPOMI). The University of Arizona also conducted facility-oriented flights in July and September 2021. These and the CU/UMD flights in 2021 were part of a State of Colorado initiative to track O&G impacts (Colorado Department of Natural Resources Oil and Gas Conservation Commission, 2022).

When the flux or basin emission estimates are arranged on a timeline as shown in Figure S3, these show no statistically significant change in methane emissions from 2012 to 2021 in contrast to the results of Reddy and Taylor (2022). For a regression against year: p=0.2 and VS-MPR =1.1. Where available, uncertainty estimates reported for each study (standard deviations) were doubled to represent the 95% confidence interval for each, and these and the AIRS DDJB methane enhancement are also plotted. While the flux numbers by themselves may present a compelling argument that O&G emissions have not changed, there are many reasons for viewing a resulting trend with caution.

Possible issues include the following: (1) Inherent (Angevine et al., 2020) and reported uncertainties in top-down flux studies are large. (2) Recent work suggests that methane emissions in O&G fields can vary dramatically on daily, weekly, and monthly time scales (Varon et al., 2022; Veefkind et al., 2022). Varon et al. (2022), for example, report that new well development and local natural gas prices were statistically significant predictors of weekly emissions in the Permian Basin in Texas, a wet gas field similar to the DJ Basin. (3) Studies in the DM/NFR are based on very limited sampling periods that are likely insufficient to capture true long-term trends given the expected short and medium-term temporal variability of methane. (4) The TROPOMI inversion analysis is based on a possibly flawed application of the Stochastic Time-Inverted Lagrangian Transport (STILT) model in the DM/NFR (model described by Lin et al., 2003; Fasoli et al., 2018) and an uncertain use of mesoscale meteorological modeling to drive STILT. In addition, there are potential issues associated with the absence of TROPOMI methane retrievals over the mountainous regions of Colorado (see de Gouw et al., 2020, for gaps in TROPOMI methane coverage in Colorado).

These studies also represent a variety of approaches to estimating flux. While the two NOAA flight campaigns and the CU/UMD study use very similar approaches and mass balance methods, the driving survey and TROPOMI inversions use substantially distinct methodologies. What effects do differences in study design and methods have on the uncertainties in a trend based on the inclusion of each set of results?

One major area of concern is the representation of meteorology in satellite inversions in the DM/NFR. Cusworth et al. (2022) report that the STILT model was only run for levels up to 1,000 m above ground level (AGL). In this application STILT accounts for surface source influences on total TROPOMI column mean methane, and a reasonable accounting of the spatial origins of methane in the column is necessary for accurate inversion results. They assumed that above 1,000 m AGL, surface source influences would be insignificant. Summer mean mixing heights over the DM/NFR are 4,000 to 5,000 m above sea level (MSL) or 2,500 m to 3,500 m AGL over the plains (Reddy and Taylor, 2022). Observed afternoon mixing heights were up to 2,500 m AGL for the FRAPPÉ 2014 summer field campaign (Kaser et al., 2017). Mountain-plains solenoid circulations can carry trace gases westward into the mountains, loft these over the

boundary layer or to the top of the boundary layer and return them to the plains at high elevations (Pfister and Reddy et al., 2017; Sullivan et al., 2016). In addition, trace gases from local and distant sources can reside in elevated residual layers.

As Kaser et al. (2017) demonstrated for O_3 in the DM/NFR, significant concentrations of trace gases from local recirculation can be present in the residual layer after the collapse of the boundary layer the previous night. These can be entrained into the local boundary layer the next day. This highlights the importance of tracking the previous day's contributions to today's column averages. Methane from the Uintah Basin in Utah and Piceance Basin in western Colorado can also be transported aloft and eastward across the mountains into the column (see Figure S4 and S5 which also show the effects of deep vertical mixing on O&G tracer concentrations). It would seem that the STILT model should be run for levels up to at least 2,500 m to 3,500 m AGL to account for these processes. What are the implications of the lack of TROPOMI retrievals over the mountains? How does this affect the spatial accounting of surface contributions to column averages as well as calculations of background?

Their estimates of the contributions of the meteorological modeling to flux uncertainty are based on modeling in simple terrain in north-central Texas (Turner et al., 2018). Meteorology will often vary dramatically from location to location within the DM/NFR because of the complex local terrain. In addition to mountain-plains solenoid circulations, other terrain-driven circulations such as the Denver Cyclone (Vu et al., 2016; Pfister et al., 2017b; Flocke et al., 2020; Reddy an Pfister, 2016) can lead to complex transport in and near the study area. For these reasons, models may be less accurate here than over simpler terrain. Meteorological model performance evaluations may be necessary for a more complete assessment of study results (see for example Pfister and Reddy et al., 2017), and these should be included in TROPOMI methane inversion studies for this area. Appropriate performance measures should be identified. What is necessary to limit uncertainties in the DM/NFR? Can meteorological model performance indicators be used to screen retrievals for inclusion in a study? Meta-analyses of past study data, similar to those applied in medical and epidemiological research (Wang et al., 2020), might yield insights into these issues and their solutions. Full reporting of performance evaluations can clarify the value of a given study for trend and effects assessments.

A second area of concern is resolving the contributions of non-O&G methane emissions in the DM/NFR. Knowing what these contributions are and how they change over time could support the assessment of progress in reducing O_3 and achieving methane reduction goals by source sector. Petron et al. (2014) report a 25% contribution to total methane from non-O&G sources in 2012 based on two flights in May. From Peischl et al. (2018), non-O&G accounted for 25% based on two flights in March of 2015. Townsend-Small et al. (2016) report a 50% contribution to total methane from biogenic sources during July and August 2014. Based on the analysis of Reddy and Taylor (2022) for June-August 2012-2020, non-O&G sources would represent 30% of total methane in 2012 and 68% in 2020, with an assumption of no annual trend in non-O&G emissions based on CDPHE estimates (Colorado Department of Public Health and Environment, 2021). Riddick et al. (2022) found a 63% contribution for 10 days in July 2021. Cusworth et al. (2022) report a 50% contribution for a 10-day period in July of 2021 and a 21% contribution for a 10-day period in September of 2021. Emissions from cattle and manure management sources were much higher in July. Fried et al. (2022) report a 27% contribution on 1 October 2021 and 17% on 5 October 2021. How much of this large variability in study results is due to trends in

O&G emissions, trends in non-O&G emissions, differences in study designs and their uncertainties, short-term variability or seasonality in emissions, sampling period issues and study geography, or errors in methodologies?

A consideration of all the coherent correlation results and metrics discussed in this paper suggests that annual or summer-average non-O&G methane emissions may be relatively constant from 2012-2020. The AIRS methane retrievals represent ~70 retrieval-days each summer (Reddy and Taylor, 2022) and more consistent and complete temporal coverage than the top-down studies. Retrievals respond to methane from all methane sources in the DDJB and DM/NFR. Ethane is primarily from O&G activities (as reported in the literature and summarized by Reddy and Taylor, 2022). Given the 0.96 correlation between the two and the strong linear relationship with a 931 to 1 probability versus the null hypothesis, it seems unlikely that there is significant year-to-year variability in non-O&G methane. Otherwise, the correlation between AIRS DDJB methane enhancement and ethane would be weaker, but this should be verified. A good first step toward resolving this area of concern might be to conduct meta-analyses of past data sets and related monitoring programs and/or literature reviews to clarify the potential features and impacts of seasonality and short-term variability in emissions from cattle and manure management activities. Golston et al. (2020), for example, report that there were significant differences in methane emissions from individual concentrated animal feeding operations with repeat surveys. A review and analysis of data from historic studies might make it possible to improve strategies for assessing non-O&G contributions.

The DM/NFR has a wealth of expertise, data, monitoring, and information, and many of these issues may already be under review, but it seems that a successful analysis of future and past trends may not be possible without a careful consideration of issues raised by past studies. Understanding the short and medium-term variability of DM/NFR methane emissions, for example, would make it possible to calculate the numbers, frequencies, and timing of aircraft flights or driving surveys needed to assess long-term trends.

3.6. AIRS DDJB Methane Enhancement as an Indicator for Tracking O&G Impacts

The AIRS DDJB methane enhancement shows promise as an indicator for tracking both O&G emissions of methane and O&G VOC impacts on O_3. Reddy and Taylor (2022) demonstrated its strong relationship with methane from O&G sources. In the current study evidence for this relationship with O&G emissions has increased, and methane enhancement has been shown to have strong correlations with SIP O&G VOC emissions estimates and O_3 at northern monitors. Evidence for its strength as an indicator is summarized in Table 2 which shows correlations between methane enhancement and ethane, emissions estimates, and O_3 at FTCW and RFLAT. Correlations range from 0.88 to 0.96, and Bayesian factors show strong to decisive evidence for all pairs. AIRS data are not suitable for flux estimates but likely represent one of the simplest and most readily obtainable metrics for tracking changes.

Table 2. Pearson Correlations and Bayesian Correlation Factors for AIRS DDJB Methane Enhancement versus Platteville Ethane, SIP O&G VOC Emissions Estimates, and FTCW and RFLAT Annual Fourth Maximum 8-hour O_3.

	Correlations with AIRS DDJB Methane Enhancement			
	Sample Size (Years)	Pearson Correlation	BF_{10} with No Prior Knowledge	BF_{10} with Prior Knowledge That Correlations Are Positive
Platteville Ethane	9	0.96	465***	931***
SIP O&G VOC Emissions	10	0.88	44*	87**
FTCW O_3	7	0.96	39*	77**
RFLAT O_3	7	0.93	17*	33*
*strong evidence, ** very strong evidence, ***decisive evidence				

4 Summary and Conclusions

The Denver Metro/North Front Range (DM/NFR) region of northern Colorado is classified as a Severe and Moderate nonattainment area (NAA) for the 2008 and 2015 O_3 National Ambient Air Quality Standards (NAAQS) of 75 ppb and 70 ppb, respectively. Compliance with these standards is measured by the three-year average of the annual fourth maximum (DMAX8). The three-year average is referred to as the design value. Attainment of these standards is challenging because the DM/NFR contains a large metropolitan area with diverse urban sources of O_3 precursors as well as the Wattenberg Field O&G resource area.

Pfister and Flocke et al. (2017) indicate that mobile sources and O&G sources are the largest contributors to summer O_3, each contributing 6-10 ppb to average DMAX8 on high-concentration days in 2014. O&G sources have a greater influence in the northern portions of the DM/NFR while mobile sources have a greater influence in the southern section which includes Denver. Ramboll Environ and Alpine Geophysics, LLC. (2017) show a pronounced north-south gradient in O&G contributions to DMAX8 for a 2017 modeling case. O&G contributions on the 10 highest days at each site average 6.6 ppb at FTCW and are only 1.7 ppb at CHAT in the southern section of the NAA.

Reddy and Taylor (2022) found 55% and 73% reductions in local methane enhancement over background and ethane, respectively, from 2013-2020 using surface measurements and data from the NASA AIRS instrument. They concluded that ethane at the Platteville site in the Wattenberg Field is representative for this O&G area located within the DM/NFR, and that ~70% of area methane was from O&G sources in 2012. There is a surprising consistency between trends in O_3 SIP O&G VOC emissions, trends in Platteville median ethane, and AIRS satellite-derived methane enhancement in the DDJB. The Bayesian correlation factor BF_{10} is 9 for emissions versus methane enhancement and 39 for emissions versus ethane. This means that these interrelationships are 9 and 39 times more likely, with substantial and very strong evidence, respectively, than no connection at all. If there has been a ~70% reduction O&G VOC emissions between 2013 and 2019 that tracks well with the O_3 SIP O&G VOC emissions inventory, then

we would expect to see reductions in peak O_3, especially in those areas in the NAA where O_3 contributions from O&G emissions are high.

After removing events flagged for wildfire smoke or stratospheric intrusions, annual fourth maximum 8-hour O3 concentrations were correlated with variables related to O&G VOC emissions as well as OMI NO_2 using Bayesian methods. FTCW and RFLAT annual fourth maximum 8-hour O_3 from 2012-2019 are highly correlated with Platteville median ethane, the SIP O&G VOC emissions, AIRS DDJB methane enhancements, and annual mean OMI tropospheric NO_2 calculated for the O&G region. These correlations also have high values for the Bayesian correlation factor (BF_{10}) or the Vovk-Sellke maximum p-ratio (VS-MPR) in most instances. The BF_{10} factor of 483-966 shows that the 0.99 correlation between FTCW O_3 and Platteville ethane is decisive, proving that O_3 here has a direct linear connection with ethane, a surrogate for O&G VOC emissions. An interconnection is 483-966 times more likely than no interconnection at all and is 28 times more likely than a response to NO_2. A partial correlation was calculated for FTCW O_3 versus ethane, and this partial correlation removes the influences of NO_x as represented by OMI tropospheric NO_2. The partial correlation between FTCW O_3 and ethane is 0.96 with a strong VS-MPR of 22.8.

In contrast to partial correlations of O_3 with ethane conditioned for OMI NO_2, partial correlations between annual fourth maximum O_3 and OMI NO_2 corrected for ethane were statistically insignificant at every site with VS-MPR values of only 1.0 to 1.7, demonstrating low probabilities for an effect. For FTCW in particular, this is compelling evidence that most of the response in O_3 from 2012 to 2019 may be the result of reductions in O&G VOCs and not NO_x. Based on partial correlations, the probability of a connection between ethane and FTCW O_3 is ~23 times higher than a connection between O_3 and NO_2 (ratio of VS-MPR values = 22.8/1.0). The ~9 ppb decline in O_3 at FTCW from 2012-2019 is in the range of the estimated contribution of O&G VOCs to O_3 at this site on maximum concentration days from 2012 through 2017.

Modeled O&G source contributions to O_3 and decreases in annual fourth maximum O_3 during the study period show a pronounced decreasing gradient from FTCW to Chatfield. This is consistent with the findings of Flocke et al. (2020) and Pfister and Flocke et al. (2017) who report that O&G influences on O_3 are higher in the northern portions of the region. The 40th parallel divides the relatively disjoint distributions of NO_x sources to the south and O&G sources to north. The fact that correlations and measures of their significance also conform to this gradient is further evidence that reductions in O&G VOC emissions have affected maximum O_3 concentrations.

Interrelationships among emissions estimates, satellite-derived methane enhancements, ethane, and maximum O_3 concentrations provide coherent evidence for major reductions in local O&G VOC emissions. Platteville median ethane and SIP O&G VOC emissions declined by 67% and 64%, respectively, between 2012 and 2019. Given the linear decline in O_3 with respect to ethane at FTCW and RFLAT and robust correlation metrics at these sites for variables related to VOC emissions, it is possible that as much as 67% of the O_3 from O&G VOCs at these sites was eliminated between 2012 and 2019. Reductions in O&G VOCs are likely to have been most effective at reducing O_3 at FTCW, WCT, and RFLAT, and least effective at CHAT. Zeroing out

O&G VOCs as represented by ethane would yield annual fourth maximum O_3 of 65 ppb (±1.6 ppb) at FTCW, 61 ppb (±4.7 ppb) at WCT, and 70 ppb (± 2.6 ppb) at RFLAT.

When arranged on a timeline, top-down methane flux studies for the DM/NFR region from 2012 to 2021 show little change in emissions, and by extension suggest that O&G emissions may also have been relatively constant. There are, however, many reasons for viewing the resulting trend with caution. Key issues include the large uncertainties in top-down flux studies (Angevine et al., 2020), the potential significant variability of fluxes in O&G fields on daily, weekly, and monthly time scales (Varon et al., 2022; Veefkind et al., 2022), and the limited temporal sampling represented by these DM/NFR studies. In addition, accurate representation of complex terrain-driven meteorology in the DM/NFR is essential for accurate satellite methane inversion modeling. Because of the complex terrain in the DM/NFR region, meteorological model performance evaluations may be necessary for reliable assessments of trends using satellite methane inversions. Meta-analyses of past data sets and related monitoring programs as well as literature reviews to clarify the seasonality and short-term variability in methane emissions in the DM/NFR could also provide much of the information necessary to refine strategies for tracking long-term trends and might make it possible to calculate the numbers, frequencies, and timing of aircraft flights or driving surveys needed to assess these trends.

The AIRS DDJB methane enhancement data shows promise as an indicator for tracking emissions of methane from O&G sources and O&G VOC impacts on O_3. In the current study evidence for this relationship with O&G emissions has increased, and methane enhancement has been shown to have strong correlations with SIP O&G VOC emissions estimates, ethane, and O_3 at northern monitors. It is likely one of the simplest and most readily obtainable metrics for tracking changes.

Acknowledgments

There were no external funding sources for this work. I acknowledge the use of AIRS and OMI NO_2 data from the NASA Giovanni website, NCEP Reanalysis data from the NOAA Physical Sciences Laboratory website, monthly methane data from the NOAA Global Monitoring Laboratory website, surface ethane data from the CDPHE repository, O_3 data from the CDPHE repository and EPA, modeled 2017 source contributions to O_3 (Ramboll Environ and Alpine Geophysics, LLC., 2017) from the Cooperative Institute for Research in the Atmosphere at Colorado State University website, and online HYSPLIT back trajectories from the NOAA Air Resources Laboratory website. The continued support of these institutions for online data access makes research like this possible. I am grateful for access to FRAPPÉ WRF-ARW forecast plots provided online by NCAR which is funded by the National Science Foundation (NSF). The work of FRAPPÉ team scientists provided the background information necessary to interpret responses in O_3 to changes in O&G VOC emissions. FRAPPÉ was funded by the State of Colorado and the NSF.

Open Research

The datasets used in this study include calculated DDJB methane enhancement data for June-August and median annual Platteville ethane for 2012-2020 from a data repository (Reddy and Taylor, 2022b), AIRS Methane and OMI Tropospheric NO_2 data from the NASA Giovanni

website (https://giovanni.gsfc.nasa.gov/giovanni/), ethane, O_3, and NO_2 monitoring data from the CDPHE Air Pollution Control Division (https://www.colorado.gov/airquality/tech_doc_repository.aspx), O_3 and NO_2 data from the EPA (https://aqs.epa.gov/aqsweb/airdata/download_files.html), monthly methane data for Niwot Ridge from the NOAA Global Monitoring Laboratory (https://gml.noaa.gov/), and NCEP Reanalysis data from the NOAA Physical Sciences Laboratory (https://psl.noaa.gov/cgi-bin/data/timeseries/timeseries1.pl). HYSPLIT back trajectories were obtained through online model runs (https://www.ready.noaa.gov/HYSPLIT_traj.php). Plots of WRF-ARW O&G tracer concentrations and mixing heights in the Supporting Information document were acquired from the NCAR Atmospheric Chemistry Observations and Modeling Laboratory FRAPPÉ field catalog (http://catalog.eol.ucar.edu/frappe/model). The 2017 O_3 local source apportionment results for WCT were obtained at the Cooperative Institute for Research in the Atmosphere website: http://vibe.cira.colostate.edu/WAQS_DenverLSA/Home/AQS. Federal Register announcements of DM/NFR NAA reclassifications can be found https://www.federalregister.gov/documents/2022/10/07/2022-20458/determinations-of-attainment-by-the-attainment-date-extensions-of-the-attainment-date-and; https://www.federalregister.gov/documents/2022/10/07/2022-20460/determinations-of-attainment-by-the-attainment-date-extensions-of-the-attainment-date-and. Key datasets are available in a data repository (Reddy, 2023). Statistical calculations were completed with JASP (https://jasp-stats.org/), NCSS 8.0, and Microsoft Excel. Graphs, plots, and maps were prepared with JASP, NCSS 8.0, Surfer 12, and Excel.

References

Albores, I. S., Buchholz, R. R., Ortega, I., Emmons, L. K., Hannigan, J. W., Lacey, F., Pfister, G., Tang, W., & Worden, H. M. (2023). Continental-scale atmospheric impacts of the 2020 Western U.S. Wildfires. *Atmospheric Environment, 294*, 119436. https://doi.org/10.1016/j.atmosenv.2022.119436

Angevine, W. M., Peischl, J., Crawford, A., Loughner, C. P., Pollack, I. B., Thompson, C. R. (2020). Errors in top-down estimates of emissions using a known source. *Atmospheric Chemistry and Physics, 20*. https://doi.org/10.5194/acp-20-11855-2020

Barna, M., Lamb, B., & Westberg, H. (2001). Modeling the effects of VOC/NOx emissions on ozone synthesis in the Cascadia Airshed of the Pacific Northwest. *Journal of the Air & Waste Management Association*, *51*(7), 1021–1034. https://doi.org/10.1080/10473289.2001.10464330

Choi, S., Lamsal, L. N., Follette-Cook, M., Joiner, J., Krotkov, N. A., Swartz, W. H., Pickering, K. E., Loughner, C. P., Appel, W., Pfister, G., Saide, P. E., Cohen, R. C., Weinheimer, A. J., & Herman, J. R. (2020). Assessment of NO_2 observations during DISCOVER-AQ and KORUS-AQ field campaigns. *Atmospheric Measurement Techniques*, *13*(5), 2523–2546. https://doi.org/10.5194/amt-13-2523-2020

Colorado Department of Natural Resources Oil and Gas Conservation Commission. (2022). Report on the evaluation of cumulative impacts, Rule 904.a. https://cogcc.state.co.us/documents/library/Cumulative_Impacts/2021_COGCC_CI_Report_20220114.pdf

Colorado Department of Public Health and Environment. (2021). Colorado 2021 Greenhouse gas inventory update with historical emissions from 2005 to 2019 and projections to 2050. Retrieved from https://drive.google.com/file/d/1SFtUongwCdZvZEEKC_VEorHky267x_np/view

Colorado Department of Public Health and Environment Air Pollution Control Division. (2022a). Colorado air quality data report 2021. https://www.colorado.gov/airquality/tech_doc_repository.aspx?action=open&file=2021AnnualDataReport.pdf

Colorado Department of Public Health and Environment Air Pollution Control Division. (2022b). State of Colorado oil and gas and point source emissions inventory development supporting the Denver Metro/North Front Range State Implementation Plan for the 2015 8-hour ozone national ambient air quality standard. APCD_FINAL_TSD-005. https://drive.google.com/drive/u/0/folders/1hTa2jj3zA4q4XEdrh2t_YLbUuBEcfruc

Crawford, J. H., & Pickering, K. E. (2014). Discover-AQ: Advancing strategies for air quality observations in the next decade. *EM Air and Waste Management Association, 9*, 4– 7. Retrieved from https://pubs.awma.org/flip/EM-Sept-2014/coverstory.pdf

Cusworth, D. H., Thorpe, A. K., Ayasse, A. K., Stepp, D., Heckler, J., Asner, G. P., Miller, C. E., Yadav, V., Chapman, J. W., Eastwood, M. L., Green, R. O., Hmiel, B., Lyon, D. R., & Duren, R. M. (2022). Strong methane point sources contribute a disproportionate fraction of total emissions across multiple basins in the United States. *Proceedings of the National Academy of Sciences, 119*(38), e2202338119. https://doi.org/10.1073/pnas.2202338119

de Gouw, J. A., Veefkind, J. P., Roosenbrand, E., Dix, B., Lin, J. C., Landgraf, J., & Levelt, P. F. (2020). Daily satellite observations of methane from oil and gas production regions in the United States. *Scientific Reports*, *10*(1), Article 1. https://doi.org/10.1038/s41598-020-57678-4

Dlugokencky, E. J., Crotwell, A. M., Mund, J. W., Crotwell, M. J., & Thoning, K. W. (2021). Atmospheric methane dry air mole fractions from the NOAA GML carbon cycle cooperative global air sampling network, 1983-2020, Version: 2021-07-30. https://doi.org/10.15138/VNCZ-M766

Fasoli, B., Lin, J. C., Bowling, D. R., Mitchell, L., & Mendoza, D. (2018). Simulating atmospheric tracer concentrations for spatially distributed receptors: Updates to the Stochastic Time-Inverted Lagrangian Transport model's R interface (STILT-R version 2). *Geoscientific Model Development*, *11*(7), 2813–2824. https://doi.org/10.5194/gmd-11-2813-2018

Flocke, F., Pfister, G., Crawford, J. H., Pickering, K. E., Pierce, G., Bon, D., & Reddy, P. (2020). Air quality in the northern Colorado Front Range metro area: The Front Range Air Pollution and Photochemistry Éxperiment (FRAPPÉ). *Journal of Geophysical Research: Atmospheres, 125*(2), e2019JD031197. https://doi.org/10.1029/2019JD031197

Flynn, Margot T., Mattson, Erick J., Jaffe, Daniel A., Gratz, Lynne E. (2021). Spatial patterns in summertime surface ozone in the Southern Front Range of the U.S. Rocky Mountains. *Elementa: Science of the Anthropocene 21*. https://doi.org/10.1525/elementa.2020.00104

Fried, Alan, Dickerson, Russell, Daley, Hannah, Stratton, Phillip, Weibring, Petter, Richter, Dirk, Walega, James, Koss, Abigail, Kimmel, Joel, Ren, Xinrong. (2022). Interim report on proposal activities and no-cost extension request: continuous airborne measurements and

887 analysis of oil & natural gas emissions during the 2021 Denver-Julesburg Basin studies. Prepared
888 for the Colorado Oil and Gas Conservation Commission and the Colorado Air Pollution Control
889 Division, Colorado Department of Public Health and Environment.
890 https://www.colorado.gov/airquality/tech_doc_repository.aspx?action=open&file=airborne_mea
891 sure_denver_julesburg_2021_report.pdf

892 Goldberg, D. L., Anenberg, S. C., Kerr, G. H., Mohegh, A., Lu, Z., & Streets, D. G. (2021).
893 TROPOMI NO_2 in the United States: A detailed look at the annual averages, weekly cycles,
894 effects of temperature, and correlation with surface NO_2 concentrations. *Earth's future*, *9*(4),
895 e2020EF001665. https://doi.org/10.1029/2020EF001665

896 Golston, L. M., Pan, D., Sun, K., Tao, L., Zondlo, M. A., Eilerman, S. J., Peischl, J., Neuman, J.
897 A., & Floerchinger, C. (2020). Variability of ammonia and methane emissions from animal
898 feeding operations in Northeastern Colorado. *Environmental Science & Technology*, *54*(18),
899 11015–11024. https://doi.org/10.1021/acs.est.0c00301

900 Kalnay, E., Kanamitsu, M., Kistler, R., Collins, W., Deaven, D., Gandin, L., et al. (1996). The
901 NCEP/NCAR 40-year reanalysis project. *Bulletin of the American Meteorological Society, 77*(3),
902 437–472. https://doi.org/10.1175/1520-0477(1996)077<0437:TNYRP>2.0.CO;2

903 Kaser, L., Patton, E. G., Pfister, G. G., Weinheimer, A. J., Montzka, D. D., Flocke,
904 F., Thompson, A. M., Stauffer, R. M., and Halliday, H. S. (2017), The effect of entrainment
905 through atmospheric boundary layer growth on observed and modeled surface ozone in the
906 Colorado Front Range, *J. Geophys. Res. Atmos., 122*, 6075– 6093,
907 https://doi.org/10.1002/2016JD026245.

908 Kass, R. E., & Raftery, A. E. (1995). Bayes factors. *Journal of the American Statistical*
909 *Association*, *90*(430), 773–795. https://doi.org/10.1080/01621459.1995.10476572

910 Kelter, R. (2020). Bayesian alternatives to null hypothesis significance testing in biomedical
911 research: a non-technical introduction to Bayesian inference with JASP. *BMC Medical Research*
912 *Methodology 20*, 142 (2020). https://doi.org/10.1186/s12874-020-00980-6

913 Krotkov, N. A., Lamsal, L. N., Celarier, E. A., Swartz, W. H., Marchenko, S. V., Bucsela, E. J.,
914 Chan, K. L., Wenig, M., & Zara, M. (2017). The version 3 OMI NO2 standard product. *Atmos.*
915 *Meas. Tech., 10*(9), 3133–3149. https://doi.org/10.5194/amt-10-3133-2017

916 Krotkov, N.A., Lamsal, L. M., Marchenko, S. V., Celarier, E. A., Bucsela, E. J., Swartz, W. H.,
917 Joiner, J., and the OMI core team. (2019). OMI/Aura NO2 cloud-screened total and tropospheric
918 column l3 global gridded 0.25 degree x 0.25 degree V3, NASA Goddard Space Flight Center,
919 Goddard Earth Sciences Data and Information Services Center (GES DISC), Accessed:
920 September, 2022, https://doi.org/10.5067/Aura/OMI/DATA3007

921 Laughner, J. L., Cohen, R. C. (2019). Direct observation of changing NOx lifetime in North
922 American cities. *Science*, *366*(6466), 723–727. https://doi.org/10.1126/science.aax6832

923 Lin, J. C., Gerbig, C., Wofsy, S. C., Andrews, A. E., Daube, B. C., Davis, K. J., & Grainger, C.
924 A. (2003). A near-field tool for simulating the upstream influence of atmospheric observations:
925 The Stochastic Time-Inverted Lagrangian Transport (STILT) model. *Journal of Geophysical*
926 *Research: Atmospheres*, *108*(D16). https://doi.org/10.1029/2002JD003161

927 Lyu, C., Capps, S. L., Kurashima, K., Henze, D. K., Pierce, G., Hakami, A., et al. (2021).
928 Evaluating oil and gas contributions to ambient nonmethane hydrocarbon mixing ratios and
929 ozone-related metrics in the Colorado Front Range. *Atmospheric Environment, 246*, 118113.
930 https://doi.org/10.1016/j.atmosenv.2020.118113

931 McDuffie, E. E., Edwards, P. M., Gilman, J. B., Lerner, B. M., Dubé, W. P., Trainer, M., Wolfe,
932 D. E., Angevine, W. M., deGouw, J., Williams, E. J., Tevlin, A. G., Murphy, J. G., Fischer, E.
933 V., McKeen, S., Ryerson, T. B., Peischl, J., Holloway, J. S., Aikin, K., Langford, A. O., …
934 Brown, S. S. (2016). Influence of oil and gas emissions on summertime ozone in the Colorado
935 Northern Front Range. *Journal of Geophysical Research: Atmospheres*, *121*(14), 8712–8729.
936 https://doi.org/10.1002/2016JD025265

937 Nuzzo, R.L. (2017), An introduction to Bayesian data analysis for correlations. *PM&R, 9*: 1278-
938 1282. https://doi.org/10.1016/j.pmrj.2017.11.003

939 Paraschiv, S., Constantin, D.-E., Paraschiv, S.-L., & Voiculescu, M. (2017). OMI and ground-
940 based in-situ tropospheric nitrogen dioxide observations over several important European cities
941 during 2005–2014. *International Journal of Environmental Research and Public Health*, *14*(11),
942 Article 11. https://doi.org/10.3390/ijerph14111415

943 Peischl, J., Eilerman, S. J., Neuman, J. A., Aikin, K. C., de Gouw, J., Gilman, J. B., et al. (2018).
944 Quantifying methane and ethane emissions to the atmosphere from central and Western U.S. oil
945 and natural gas production regions. *Journal of Geophysical Research: Atmospheres, 123*, 7725–
946 7740. https://doi.org/10.1029/2018JD028622

947 Pétron, G., Karion, A., Sweeney, C., Miller, B. R., Montzka, S. A., Frost, G. J., et al. (2014). A
948 new look at methane and nonmethane hydrocarbon emissions from oil and natural gas operations
949 in the Colorado Denver-Julesburg Basin. *Journal of Geophysical Research: Atmospheres,*
950 *119*(11), 6836– 6852. https://doi.org/10.1002/2013JD021272

951 Pfister, G. G., Reddy, P. J., Barth, M. C., Flocke, F. F., Fried, A., Herndon, S. C., et al. (2017).
952 Using observations and source-specific model tracers to characterize pollutant transport during
953 FRAPPÉ and DISCOVER-AQ. *Journal of Geophysical Research: Atmospheres, 122*(19),
954 10510– 10538. https://doi.org/10.1002/2017JD027257

955 Pfister, Gabriele, Flocke, Frank, Hornbrook, Rebecca, Orlando, John, Lee, Sojin, Schroeder,
956 Jason. (2017). Process-based and regional source impact analysis for FRAPPÉ and DISCOVER-
957 AQ 2014. National Center for Atmospheric Research.
958 https://www.colorado.gov/airquality/tech_doc_repository.aspx?action=open&file=FRAPPE-
959 NCAR_Final_Report_July2017.pdf

960 Pfister, G., Wang, C.-T., Barth, M., Flocke, F., Vizuete, W., & Walters, S. (2019). Chemical
961 characteristics and ozone production in the Northern Colorado Front Range. *Journal of*
962 *Geophysical Research: Atmospheres, 124*, 13397– 13419.
963 https://doi.org/10.1029/2019JD030544

964 Ramboll Environ and Alpine Geophysics, LLC. (2017). Denver Metro/North Front Range local
965 source 2017 ozone source apportionment modeling using a 2011 modeling database. prepared for
966 the Regional Air Quality Council.
967 https://raqc.egnyte.com/dl/VxMTx5309z/Denver_2017_SA_Rpt_v6_2017-04-12-FINAL.pdf_

968 Reddy, P. J., & Pfister, G. G. (2016). Meteorological factors contributing to the interannual
969 variability of midsummer surface ozone in Colorado, Utah, and other Western U.S. states.
970 *Journal of Geophysical Research: Atmospheres, 121*(5), 2434– 2456.
971 https://doi.org/10.1002/2015JD023840

972 Reddy, P. J., Parker, L. K., Morris, R. (2020). Trends in weather corrected ozone and nitrogen
973 dioxide updated through 2019. Prepared for the Regional Air Quality Council, Ramboll US
974 Corporation,
975 https://raqc.egnyte.com/dl/XBdOYH6zjc/TSD_Weather_Corrected_Trends_Report_v3.pdf_

976 Reddy, P. J., & Taylor, C. (2022). Downward trend in methane detected in a northern Colorado
977 oil and gas production region using AIRS satellite data. *Earth and Space Science*, 9,
978 e2022EA002609. https://doi.org/10.1029/2022EA002609

979 Reddy, P. J., & Taylor, C. (2022b). Downward trend in methane detected in a Northern Colorado
980 oil and gas production region using AIRS satellite data. (Version 1) [Dataset]. Zenodo.
981 https://doi.org/10.5281/zenodo.7038756

982 Reddy, P. J. (2023). Synthesis of satellite and surface measurements, model results, and
983 FRAPPÉ study findings to assess the impacts of oil and gas emissions reductions on maximum
984 ozone in the Denver Metro and Northern Front Range region in Colorado (Version 1) [Data set].
985 Zenodo. https://doi.org/10.5281/zenodo.7686196

986 Regional Air Quality Council. (2022). Draft executive summary of the moderate area ozone SIP
987 for the 2015 ozone NAAQS. Retrieved from
988 https://raqc.egnyte.com/dl/mzt7ZQmmad/DRAFTRAQCBoardSIPExecutiveSummary2015.pdf_

989 Riddick, S.N., Cheptonui, F., Yuan, K., Mbua, M., Day, R., Vaughn, T.L., Duggan, A., Bennett,
990 K.E., Zimmerle, D.J. (2022) Estimating regional methane emission factors from energy and
991 agricultural sector sources using a portable measurement system: case study of the Denver–
992 Julesburg Basin. *Sensors, 22*. https://doi.org/10.3390/s22197410

993 Rolph, G., Stein, A., & Stunder, B. (2017). Real-time environmental applications and display
994 system: Ready. *Environmental Modelling & Software, 95*, 210– 228.
995 https://doi.org/10.1016/j.envsoft.2017.06.025

996 Ruiz-Ruano García, A. M., & López Puga, J. (2018). Deciding on null hypotheses using p-values
997 or Bayesian alternatives: a simulation study. *Psicothema, 30*(1), 110–115.
998 https://doi.org/10.7334/psicothema2017.308

999 Sellke, T., Bayarri, M. J., & Berger, J. O. (2001). Calibration of p values for testing precise null
1000 hypothesis. *The American Statistician, 55*, 62-71. https://doi.org/10.7334/psicothema2017.308

1001 Stein, A. F., Draxler, R. R., Rolph, G. D., Stunder, B. J. B., Cohen, M. D., & Ngan, F. (2015).
1002 NOAA's HYSPLIT atmospheric transport and dispersion modeling system. *Bulletin of the*
1003 *American Meteorological Society, 96*(12), 2059– 2077. https://doi.org/10.1175/BAMS-D-14-
1004 00110.1

Sullivan, J. T., McGee, T. J., Langford, A. O., Alvarez II, R. J., Senff, C. J., Reddy, P. J., Thompson, A. M., Twigg, L. W., Sumnicht, G. K., Lee, P., Weinheimer, A., Knote, C., Long, R. W., & Hoff, R. M. (2016). Quantifying the contribution of thermally driven recirculation to a high-ozone event along the Colorado Front Range using lidar. *Journal of Geophysical Research: Atmospheres*, *121*(17), 10,377-10,390. https://doi.org/10.1002/2016JD025229

Thrastarson, H. D., Manning, E., Kahn, B., Fetzer, E. J., Yue, Q., Wong, S., et al. (2021). AIRS/AMSU/HSB Version 7 Level 2 product user guide. Jet Propulsion Laboratory. Retrieved from https://docserver.gesdisc.eosdis.nasa.gov/public/project/AIRS/V7_L2_Product_User_Guide.pdf

Toth, J. J., & Johnson, R. H. (1985). Summer surface flow characteristics over northeast Colorado. *Monthly Weather Review, 113*(9), 1458– 1469. https://doi.org/10.1175/1520-0493(1985)113<1458:SSFCON>2.0.CO;2

Townsend-Small, A., Botner, E. C., Jimenez, K. L., Schroeder, J. R., Blake, N. J., Meinardi, S., Blake, D. R., Sive, B. C., Bon, D., Crawford, J. H., Pfister, G., Flocke, F. M. (2016), Using stable isotopes of hydrogen to quantify biogenic and thermogenic atmospheric methane sources: A case study from the Colorado Front Range, *Geophys. Res. Lett., 43*, 11,462– 11,471, https://doi.org/10.1002/2016GL071438

Turner, A. J., Jacob, D. J., Benmergui, J., Brandman, J., White, L., Randles, C. A. (2018). Assessing the capability of different satellite observing configurations to resolve the distribution of methane emissions at kilometer scales, *Atmos. Chem. Phys., 18*, 8265–8278, https://doi.org/10.5194/acp-18-8265-2018

Varon, D. J. and Jacob, D. J. and Hmiel, B. and Gautam, R. and Lyon, D. R. and Omara, M. and Sulprizio, M. and Shen, L. and Pendergrass, D. and Nesser, H. and Qu, Z. and Barkley, Z. R. and Miles, N. L. and Richardson, S. J. and Davis, K. J. and Pandey, S. and Lu, X. and Lorente, A. and Borsdorff, T. and Maasakkers, J. D. and Aben, I. (2022). Continuous weekly monitoring of methane emissions from the Permian Basin by inversion of TROPOMI satellite observations. (Preprint). *Atmospheric Chemistry and Physics Discussions*. https://acp.copernicus.org/preprints/acp-2022-749/

Vazquez Santiago, J., Inoue, K., & Tonokura, K. (2021). Diagnosis of ozone formation sensitivity in the Mexico City Metropolitan Area using HCHO/NO2 column ratios from the ozone monitoring instrument. *Environmental Advances*, *6*, 100138. https://doi.org/10.1016/j.envadv.2021.100138

Veefkind, J. P., Serrano-Calvo, R., de Gouw, J. A., Dix, B. K., Schneising, O., Buchwitz, M., Barré, J. E., van der A, R. J., Liu, M., & Levelt, P. F. (2022). Continuous methane emissions from the oil and gas industry in the Permian Basin [Preprint]. *Atmospheric Sciences*. https://doi.org/10.1002/essoar.10512099.1

Vu, K. T., Dingle, J. H., Bahreini, R., Reddy, P. J., Apel, E. C., Campos, T. L., DiGangi, J. P., Diskin, G. S., Fried, A., Herndon, S. C., Hills, A. J., Hornbrook, R. S., Huey, G., Kaser, L., Montzka, D. D., Nowak, J. B., Pusede, S. E., Richter, D., Roscioli, J. R., … Flocke, F. (2016). Impacts of the Denver Cyclone on regional air quality and aerosol formation in the Colorado Front Range during FRAPPÉ 2014. *Atmospheric Chemistry and Physics*, *16*(18), 12039–12058. https://doi.org/10.5194/acp-16-12039-2016

1047 Wang, X.-M., Zhang, X.-R., Li, Z.-H., Zhong, W.-F., Yang, P., & Mao, C. (2021). A brief
1048 introduction of meta-analyses in clinical practice and research. *The Journal of Gene Medicine,*
1049 *23*(5), e3312. https://doi.org/10.1002/jgm.3312

1050

Submitted to *Earth and Space Science*

Supporting Information for

Synthesis of Satellite and Surface Measurements, Model Results, and FRAPPÉ Study Findings to Assess the Impacts of Oil and Gas Emissions Reductions on Maximum Ozone in the Denver Metro and Northern Front Range Region in Colorado

P. J. Reddy[1]

[1]Independent Research Scientist, Crestone, Colorado

Contents of this file

Text S1 to S5
Figures S1 to S5

Introduction

Supplementary figures and supporting text referenced in the paper are presented here as well as a relisting of the references for information in Figure S3. The figure captions are listed below:

Figure S1. Linear regressions of annual average OMI Tropospheric NO_2 versus year for 2010-2019 with 95% confidence limits for Urban area (inverted orange triangles) and O&G area (green triangles) as defined in the paper. LOESS smoothing curves are also plotted.

Figure S2 Linear regressions of annual fourth maximum 8-hour O3 in ppb (ranked after removal of events flagged for smoke or stratospheric intrusions) versus year at RFLAT, NREL, CHAT, WCT, and FTCW for 2011-2019 as described in the body of the main paper.

Figure S3. Methane fluxes (10^6 g/hr) in the DM/NFR region from aircraft studies, a driving survey, and TROPOMI methane inversions, and AIRS DDJB methane enhancement in ppb.

TROPOMI inversions are in red, aircraft studies in blue, methane enhancement in yellow, and the driving survey is plotted with a green circle. Two sigma intervals (95% confidence intervals) are plotted with green bars for studies that report uncertainties.

Figure S4. O&G tracer concentrations in ppb modeled with the NCAR ACOM WRF-ARW during the FRAPPÉ Field experiment for 6:00 GMT 28 July 2014 at latitudes from 38.5°N to 40.5°N, showing emissions from the Uintah and Piceance Basins, on the left sides of the lower left and upper right panels, respectively, and the DM/NFR (black dot). The planetary boundary layer height is shown with a purple line.

Figure S5. O&G tracer concentrations in ppb modeled with the NCAR ACOM WRF-ARW during the FRAPPÉ field experiment for 20:00 GMT 12 July 2014 at latitudes from 38.5°N to 40.5°N, showing emissions from the Uintah and Piceance Basins, on the left sides of the lower left and upper right panels, respectively, and the DM/NFR (black dot). The planetary boundary layer height is shown with a purple line.

Text S1.

Linear regressions of annual average OMI Tropospheric NO_2 versus year for 2010-2019 with 95% confidence limits for the Urban area (inverted triangles) and O&G area (green triangles) as defined in the paper. Negative values were removed prior to averaging. The R^2 for the Urban area is 0.67 and for the O&G area it is 0.61. The null hypothesis that the slope is zero is rejected for each area. LOESS smoothing curves with a smoothing parameter of 0.55 are also shown. Based on the regressions, Urban area NO_2 declined 22% and O&G area NO_2 declined 11% from 2012-2019. See the main paper for data sources.

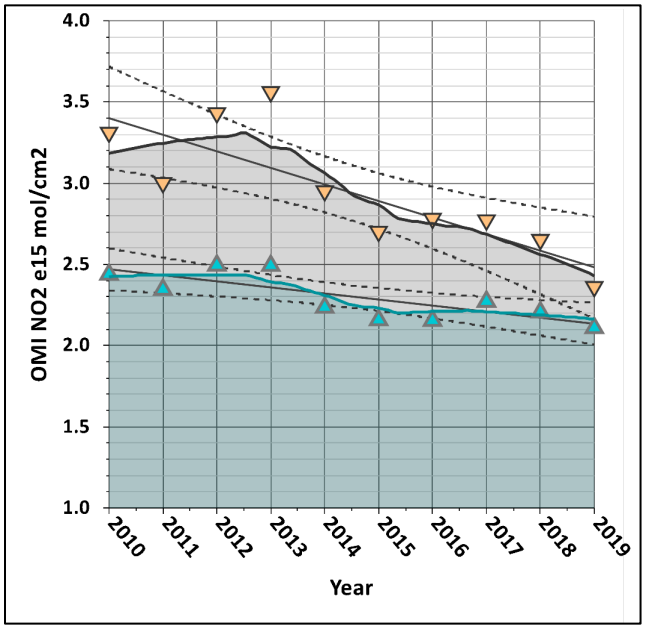

Figure S1. Linear regressions of annual average OMI Tropospheric NO_2 versus year for 2010-

2019 with 95% confidence limits for Urban area (inverted orange triangles) and O&G area (green triangles) as defined in the paper. LOESS smoothing curves are also plotted.

Text S2.

Linear regressions of annual fourth maximum 8-hour O_3 in ppb (ranked after removal of events flagged for smoke or stratospheric intrusions) versus year at FTCW, WCT, RFLAT, NREL, and CHAT for 2011-2019 as described in the main paper. Outliers having studentized residuals greater than or equal to 2.5 as determined by regressing O_3 against year were removed for WCT and RFLAT. R^2 values are 0.90, 0.48, 0.20, 0.93, and 0.89 for RFLAT, NREL, CHAT, WCT, and FTCW, respectively. The null hypothesis that the slope is zero is rejected for each site except CHAT. See the main paper for data sources.

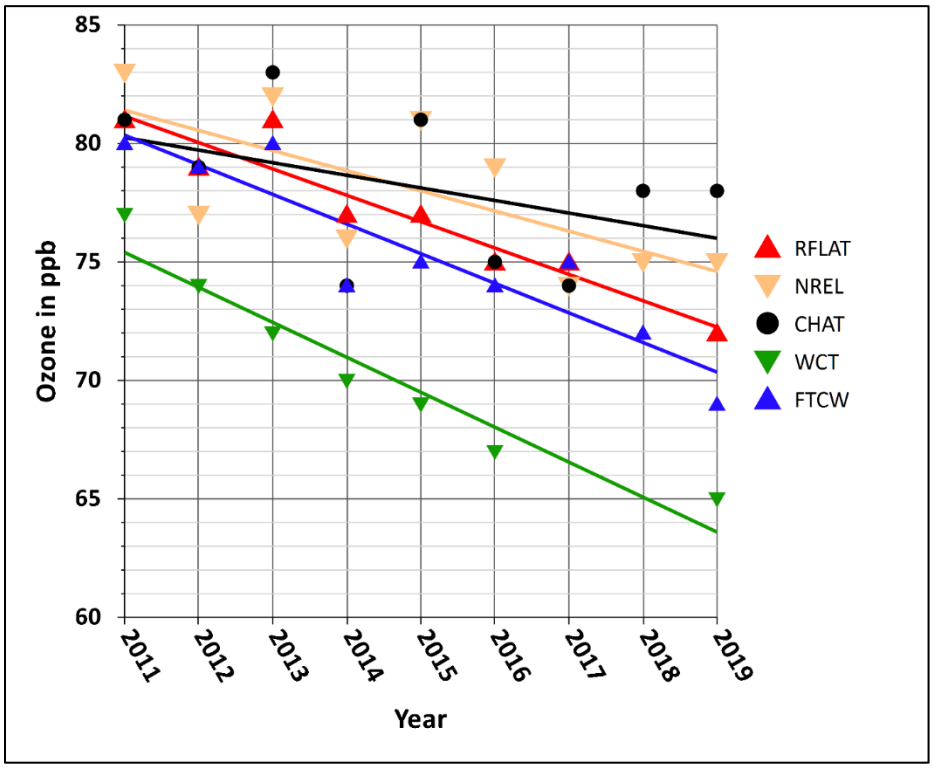

Figure S2. Linear regressions of annual fourth maximum 8-hour O3 in ppb (ranked after removal of events flagged for smoke or stratospheric intrusions) versus year at RFLAT, NREL, CHAT, WCT, and FTCW for 2011-2019 as described in the body of the main paper.

Text S3.

Methane fluxes (10^6 g/hour) in the DM/NFR region from aircraft studies, a driving survey, and TROPOMI methane inversions, and AIRS DDJB methane enhancement in ppb (Reddy and Taylor, 2022 and 2022b). These include flux estimates based on two NOAA flights in late May 2012 (Petron et al., 2014), two NOAA flights in March 2015 (Peischl et al., 2018), two University of Colorado (CU) and University of Maryland (UMD) flights in early October 2021 (Fried et al., 2022), a driving survey in the summer of 2021 (Riddick et al., 2022), and a University of Arizona

satellite methane inversion analysis for June-July and September-October 2021 (Cusworth et al., 2022). The inversions used column-average methane concentrations retrieved from the TROPOspheric Monitoring Instrument (TROPOMI). The 15.7 10^6 g/hour flux plotted for the driving survey (Riddick et al., 2022) represents the sum of their totals for O&G and agricultural sources (6.4 10^6 g/hour and 7.9 10^6 g/hour, respectively) divided by the sum of the proportions of the total flux for each (0.37 + 0.54).

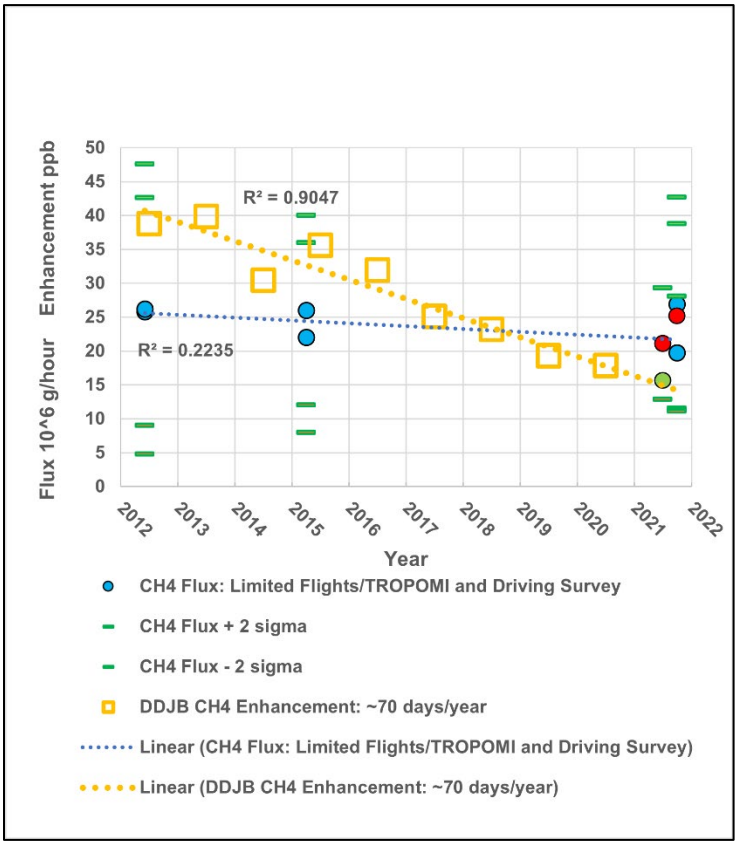

Figure S3. Methane fluxes (10^6 g/hr) in the DM/NFR region from aircraft studies, a driving survey, and TROPOMI methane inversions, and AIRS DDJB methane enhancement in ppb. TROPOMI inversions are in red, aircraft studies in blue, methane enhancement in yellow, and the driving survey flux is plotted with a green circle. Two sigma intervals (95% confidence intervals) are plotted with green bars for studies that report uncertainties.

Text S4.

O&G tracer concentrations in ppb modeled with the NCAR ACOM WRF-ARW during the FRAPPÉ Field experiment for 6:00 GMT 28 July 2014 at latitudes from 38.5°N to 40.5°N, showing emissions from the Uintah and Piceance Basins, on the left sides of the lower left and upper right panels, respectively, and the DM/NFR (black dot). Significant concentrations above the planetary boundary layer height (purple line) are present at high altitudes in the residual layer from the previous day's vertical mixing. Source: http://catalog.eol.ucar.edu/FRAPPE/model/arw_mmm_3km/trOG_WEcrosssection/20140728/0000?image_forecast_hour=008.

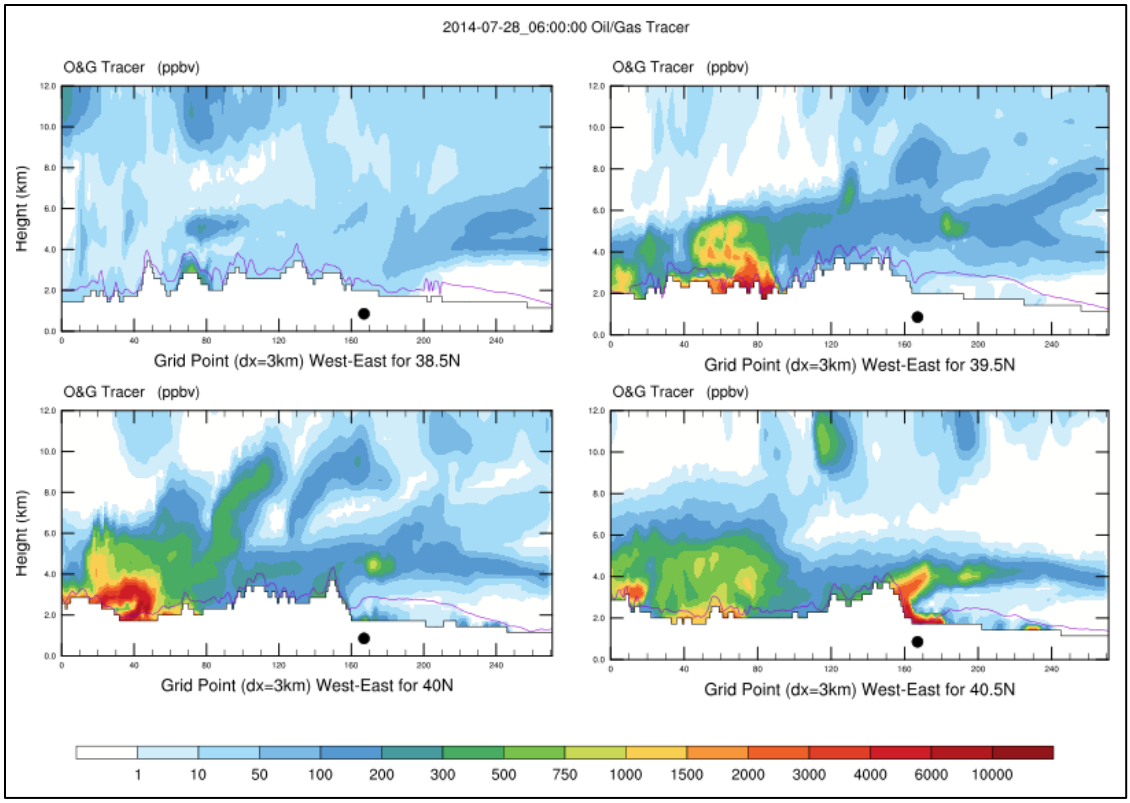

Figure S4. O&G tracer concentrations in ppb modeled with the NCAR ACOM WRF-ARW during the FRAPPÉ Field experiment for 6:00 GMT 28 July 2014 at latitudes from 38.5°N to 40.5°N, showing emissions from the Uintah and Piceance Basins, on the left sides of the lower left and upper right panels, respectively, and the DM/NFR (black dot). The planetary boundary layer height is shown with a purple line.

Text S5.

O&G tracer concentrations in ppb modeled with the NCAR ACOM WRF-ARW during the FRAPPÉ field experiment for 20:00 GMT 12 July 2014 at latitudes from 38.5°N to 40.5°N, showing emissions from the Uintah and Piceance Basins, on the left sides of the lower left and upper right panels, respectively, and the DM/NFR (black dot). Significant concentrations are present at 4,000 m MSL (~2,500 m AGL) over the DM/NFR where the planetary boundary layer height is at 5,000 to 6,000 MSL (purple line). Source: http://catalog.eol.ucar.edu/FRAPPE/model/arw_mmm_3km/trOG_WEcrosssection/20140712/1200?image_forecast_hour=006.

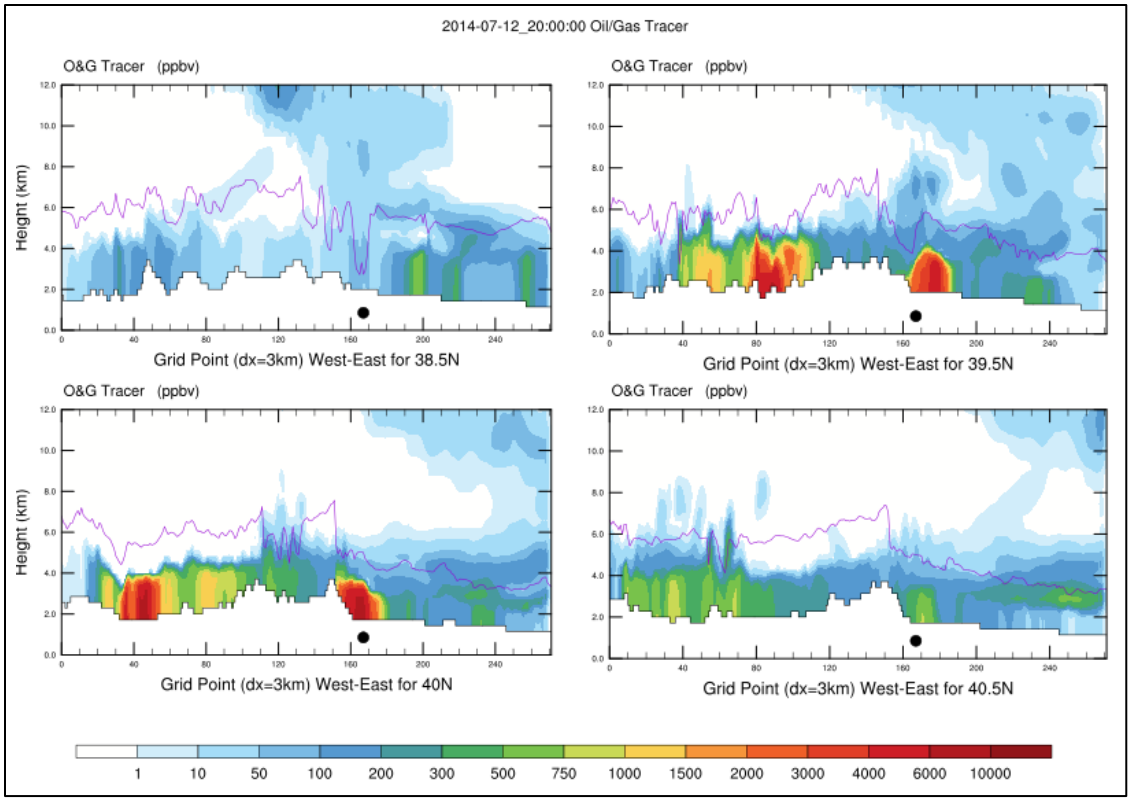

Figure S5. O&G tracer concentrations in ppb modeled with the NCAR ACOM WRF-ARW during the FRAPPÉ field experiment for 20:00 GMT 12 July 2014 at latitudes from 38.5°N to 40.5°N, showing emissions from the Uintah and Piceance Basins, on the left sides of the lower left and upper right panels, respectively, and the DM/NFR (black dot). The planetary boundary layer height is shown with a purple line.

References

Cusworth, D. H., Thorpe, A. K., Ayasse, A. K., Stepp, D., Heckler, J., Asner, G. P., Miller, C. E., Yadav, V., Chapman, J. W., Eastwood, M. L., Green, R. O., Hmiel, B., Lyon, D. R., & Duren, R. M. (2022). Strong methane point sources contribute a disproportionate fraction of total emissions across multiple basins in the United States. *Proceedings of the National Academy of Sciences, 119*(38), e2202338119. https://doi.org/10.1073/pnas.2202338119

Fried, Alan, Dickerson, Russell, Daley, Hannah, Stratton, Phillip, Weibring, Petter, Richter, Dirk, Walega, James, Koss, Abigail, Kimmel, Joel, Ren, Xinrong. (2022). Interim report on proposal activities and no-cost extension request: continuous airborne measurements and analysis of oil & natural gas emissions during the 2021 Denver-Julesburg Basin studies. Prepared for the Colorado Oil and Gas Conservation Commission and the Colorado Air Pollution Control Division, Colorado Department of Public Health and Environment. https://www.colorado.gov/airquality/tech_doc_repository.aspx?action=open&file=airborne_measure_denver_julesburg_2021_report.pdf

Peischl, J., Eilerman, S. J., Neuman, J. A., Aikin, K. C., de Gouw, J., Gilman, J. B., et al. (2018). Quantifying methane and ethane emissions to the atmosphere from central and Western U.S. oil and natural gas production regions. *Journal of Geophysical Research: Atmospheres, 123*, 7725–7740. https://doi.org/10.1029/2018JD028622

Pétron, G., Karion, A., Sweeney, C., Miller, B. R., Montzka, S. A., Frost, G. J., et al. (2014). A new look at methane and nonmethane hydrocarbon emissions from oil and natural gas operations in the Colorado Denver-Julesburg Basin. *Journal of Geophysical Research: Atmospheres, 119*(11), 6836– 6852. https://doi.org/10.1002/2013JD021272

Reddy, P. J., & Taylor, C. (2022). Downward trend in methane detected in a northern Colorado oil and gas production region using AIRS satellite data. *Earth and Space Science, 9*, e2022EA002609. https://doi.org/10.1029/2022EA002609

Reddy, P. J., & Taylor, C. (2022b). Downward trend in methane detected in a Northern Colorado oil and gas production region using AIRS satellite data. (Version 1) [Dataset]. Zenodo. https://doi.org/10.5281/zenodo.7038756

Riddick, S.N., Cheptonui, F., Yuan, K., Mbua, M., Day, R., Vaughn, T.L., Duggan, A., Bennett, K.E., Zimmerle, D.J. (2022) Estimating regional methane emission factors from energy and agricultural sector sources using a portable measurement system: case study of the Denver–Julesburg Basin. *Sensors, 22*. https://doi.org/10.3390/s22197410